LAYERED CONTENT DELIVERY OVER SATELLITE INTEGRATED COGNITIVE RADIO NETWORKS

by

Sebahat Sinem Kafıloğlu

B.S., Computer Engineering, Boğaziçi University, 2013

Submitted to the Institute for Graduate Studies in
Science and Engineering in partial fulfillment of
the requirements for the degree of
Master of Science

Graduate Program in Computer Engineering

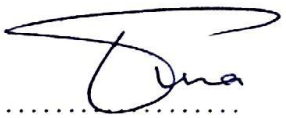
Boğaziçi University

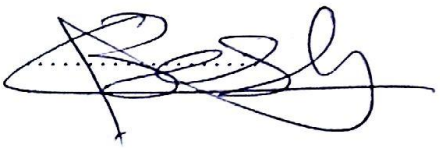
2016

LAYERED CONTENT DELIVERY OVER SATELLITE INTEGRATED COGNITIVE RADIO NETWORKS

APPROVED BY:

Prof. Fatih Alagöz ..... 
(Thesis Supervisor)

Prof. Tuna Tuğcu ..... 

Assoc. Prof. Berk Canberk ..... 

DATE OF APPROVAL: January 5, 2016

ACKNOWLEDGEMENTS

I would like to thank my thesis supervisor Prof. Fatih Alagöz for many enlightening suggestions and guidance during the development of this thesis, and helpful comments on the thesis text. Without his good will, help, and support, it would not be possible to finish this thesis.

I am grateful to Prof. Tuna Tuğcu and Assoc. Prof. Berk Canberk for their participation in my thesis committee and for their insightful and constructive comments to improve my thesis work.

I would like to offer my deepest thanks to Gürkan Gür for his mentoring, friendship, kind help, and patience.

Last, I would like to thank my family members for their patience and support through all the phases of my education.

ABSTRACT

LAYERED CONTENT DELIVERY OVER SATELLITE INTEGRATED COGNITIVE RADIO NETWORKS

Although the spectrum is a scarce and valuable resource, the utilization of spectrum in various frequency bands in certain areas are shown to be very low. Because of this under-utilization and inefficiency, cognitive radio (CR) concept where licensed bands are allowed to be used by a secondary network is being developed. Moreover, this new phenomenon has been coexisting with the exploding content consumption over wireless networks. Upcoming fifth generation (5G) wireless standards have been developed to address this capacity crunch. In 5G "toolkit", Device-to-device (D2D) communications is an important approach adopted to alleviate this issue. Moreover, heterogeneous wireless networks composed of different network tiers are expected to provide services in an omnipresent setting. In this thesis, we develop an analytical Markovian model for content delivery over satellite integrated cognitive radio networks. Additionally, we devise a simulation for studying this infrastructure-based mobile network. The simulation model is focused on energy efficiency. However, it can be extended for other performance evaluation purposes. We also investigate the effect of various system parameters on the performance of these systems such as network density, preference ratios for content retrieval from different content holders and average content size in this setting.

ÖZET

UYDULARLA TÜMLEŞİK BİLİŞSEL RADYO AĞLARINDA KATMANLI İÇERİK DAĞITIMI

Spektrum nadir ve değerli bir kaynak olmasına rağmen, belli bölgelerdeki çeşitli frekans bantlarında spektrumdan faydalanmanın oldukça düşük olduğu gösterilmiştir. Bu olgu ışığında spektrum kullanımındaki verimsizliği aşmak amacıyla lisanslı bantların ikincil bir ağ tarafından kullanılmasına izin veren bilişsel radyo kavramı geliştirilmiştir. Ayrıca, bu zorlu durum çok büyük artış gösteren kablosuz ağlar üzerinden içerik tüketimiyle eş zamanlı gerçekleşmektedir. Bu kapasite problemini çözmek için 5G kablosuz ağ standartı geliştirilmektedir. 5G teknolojilerinde Cihazdan-Cihaza İletişim bu darboğazı aşmak için seçilen önemli bir yaklaşımdır. Ayrıca bu sistemlerde farklı ağ katmanlarından oluşan heterojen kablosuz ağların her yerde gerekli servis vermeleri beklenmektedir. Bu tezde, uydularla tümleşik bilişsel radyo ağlarında içerik dağıtımı için analitik bir Markov modeli geliştirilmiştir. Ek olarak, bu tür altyapı-tabanlı mobil ağları incelemek için bir simülasyon yaklaşımı da oluşturulmuştur. Simülasyon modelimiz enerji verimliliğine odaklanmasına rağmen başka başarım değerlendirmeleri amacıyla genişletilebilir. Ayrıca söz konusu ortamda ağ yoğunluğu, farklı içerik sağlayıcılardan içerik edinimi tercih oranları ve ortalama içerik boyutu gibi çeşitli sistem parametrelerinin sistem başarımı üzerine etkileri araştırılmıştır.

TABLE OF CONTENTS

ACKNOWLEDGEMENTS . . . iii
ABSTRACT . . . iv
ÖZET . . . v
LIST OF FIGURES . . . viii
LIST OF TABLES . . . x
LIST OF SYMBOLS . . . xi
LIST OF ACRONYMS/ABBREVIATIONS . . . xvii
1. INTRODUCTION . . . 1
2. RELATED WORK . . . 5
3. CONTENT-ORIENTED SATELLITE INTEGRATED COGNITIVE RADIO NETWORK . . . 14
4. ANALYTICAL SYSTEM MODEL . . . 17
4.1. System Model . . . 17
4.2. Content Model . . . 18
4.3. Traffic Model . . . 19
4.4. Assumptions and Parameters . . . 19
4.5. State Diagram . . . 23
4.6. State Transitions . . . 24
4.6.1. PU Transitions . . . 24
4.6.2. SU Transitions . . . 27
4.6.3. HU Transitions . . . 28
4.7. Balance Equations . . . 31
4.8. Performance Metrics . . . 32
4.8.1. Throughput . . . 32
4.8.2. Energy Efficiency . . . 32
4.9. Performance Evaluation without Caching in the System . . . 33
4.9.1. Effect of Mode Preference: Satellite, BS or D2D . . . 33
4.9.2. Effect of PU Traffic Activity (Changing $\lambda_{\mathbf{PU}}^{\mathbf{ter}}$) . . . 36
4.10. Analytical Results with Integrated Caching Mechanism . . . 37

4.10.1. Effect of Mode Preference: Satellite, BS or D2D 37
4.10.2. Effect of Cache Size ($\mathbf{Cache_{HU}}$) 40
4.10.3. Effect of PU Traffic Activity (Changing $\lambda_{\mathbf{PU}}^{\mathbf{ter}}$) 41
5. SIMULATION BASED INVESTIGATION 43
5.1. Content Model 43
5.2. Traffic Model 45
5.3. Assumptions and Parameters 46
5.4. Resource Allocation 49
5.4.1. PU Arrival at the Satellite Link 49
5.4.2. PU Arrival at the Terrestrial Link 49
5.4.3. SU Arrival at the Terrestrial Link 50
5.4.4. HU Arrival 50
5.4.5. Departure 53
5.5. Energy Consumption Model 53
5.5.1. HU Device Energy States 54
5.5.2. BS Energy States 55
5.6. Quality Model 56
5.7. Experimental Results 57
5.7.1. Network Density 57
5.7.2. Effect of Mode Preference: Satellite, BS or D2D 59
5.7.3. Effect of PU Traffic Activity at Terrestrial Link (Changing $\lambda_{\mathbf{PU}}^{\mathbf{ter}}$) 65
5.7.4. Effect of Content Size 67
5.7.5. Effect of Content Popularity Characteristics 69
6. CONCLUSIONS 72
REFERENCES 74

LIST OF FIGURES

1.1 The techniques and paradigms integrated and proposed as a system in thesis work. ITSN: integrated terrestrial-satellite network . . . 3

3.1 System model. There are different operation modes based on the attached entity (satellite, BS, other device). 14

3.2 Layered content abstraction entailing base and enhancement layers. 15

4.1 State. 23

4.2 PU transitions at the satellite link. 24

4.3 PU transitions at the terrestrial link. 25

4.4 SU transitions. 27

4.5 HU transitions. 28

4.6 Effect of increasing satellite preference parameter. 34

4.7 Effect of increasing BS preference parameter. 35

4.8 Effect of increasing D2D preference parameter. 36

4.9 Effect of increasing PU arrival rate at terrestrial link. 37

4.10 Effect of increasing satellite preference parameter. 38

4.11 Effect of increasing BS preference parameter. 39

4.12 Effect of increasing D2D preference parameter. 40

4.13 Effect of increasing HU device cache size. 41

4.14 Effect of increasing PU arrival rate at terrestrial link. 42

5.1 Satellite link state x. 51

5.2 Terrestrial link state x. 51

5.3 HU device energy states. 55

5.4 BS energy states. 56

5.5 Effect of network density on the performance metrics. 58

5.6 Effect of network density. 59

5.7 Effect of increasing satellite preference parameter. 60

5.8 Effect of increasing satellite preference parameter. 61

5.9 Effect of increasing BS preference parameter. 62

5.10 Effect of increasing BS preference parameter. 63
5.11 Effect of increasing D2D preference parameter. 64
5.12 Effect of increasing D2D preference parameter. 65
5.13 Effect of increasing PU arrival rate at terrestrial link. 66
5.14 Effect of increasing PU arrival rate at terrestrial link. 67
5.15 Effect of increasing average content size. 68
5.16 Effect of increasing average content size. 69
5.17 Effect of increasing Zipf parameter α value (changing popularity characteristics). 70
5.18 Effect of increasing Zipf parameter α value (changing popularity characteristics). 71

LIST OF TABLES

4.1	Analytical parameters.	20
4.2	Analytical parameters.	21
4.3	PU transitions at the satellite link.	25
4.4	PU transitions at the terrestrial link.	26
4.5	SU transitions.	27
4.6	Content availability and preference coefficient parameters.	29
4.7	HU arrival transitions.	30
4.8	HU departure transitions.	31
5.1	Simulation parameters.	47
5.2	Simulation parameters without unit.	48
5.3	Energy model parameters.	53

LIST OF SYMBOLS

b	$\frac{(b+1)}{2}$ base contents will be located at the satellite or base station unless size exceeds corresponding cache size
c_{HU}	Hybrid user increase factor
d_{BS}	Mean distance to the base station of a primary user, secondary user and/or hybrid user
d_{sat}	Distance from satellite to earth
d_{D2D}	Mean distance between receiver and sender hybrid user devices
C_{PU}^{sat}	Channel capacity of primary user at satellite link
C_{PU}^{ter}	Channel capacity of primary user at terrestrial link
C_{SU}^{ter}	Channel capacity of secondary user at terrestrial link
C_{HU}^{sat}	Channel capacity of a hybrid user at satellite link where content is retrieved from the satellite
C_{HU}^{BS}	Channel capacity of a hybrid user at terrestrial link where content is retrieved from the base station
C_{HU}^{D}	Channel capacity of a hybrid user at terrestrial link where content is retrieved from another hybrid user device
$Cache_{sat}$	Satellite cache size
$Cache_{BS}$	Base station cache size
$Cache_{Dev}$	Hybrid device cache size
$E_{D,sw(s)}^{rec}$	Frequency switching energy of a hybrid device at satellite link for content retrieval
$E_{D,sw(t)}^{rec}$	Frequency switching energy of a hybrid device at terrestrial link for content retrieval
$E_{D,sw(t)}^{tx}$	Frequency switching energy of a hybrid device at terrestrial link for content transmission
$E_{D,sw(s->t)}^{rec}$	Mode switching energy of a hybrid device from satellite to terrestrial link for content retrieval
$E_{D,sw(s->t)}^{tx}$	Mode switching energy of a hybrid device from satellite to terrestrial link for content transmission
$E_{D,sw(t->s)}^{rec}$	Mode switching energy of a hybrid device from terrestrial to satellite link for content retrieval

$E^{rec}_{w(s)}$	Wakeup energy of a hybrid device at satellite link for content retrieval
$E^{rec}_{w(t)}$	Wakeup energy of a hybrid device at terrestrial link for content retrieval
$E^{tx}_{w(t)}$	Wakeup energy of a hybrid device at terrestrial link for content transmission
$E_{w(idle)}$	Wakeup energy of a hybrid device to the idle state
EE_{HU}	Energy efficiency of hybrid users
EPB_{HU}	Energy consumption of per each successfully sent bit for hybrid users
f_{sat}	Frequency of satelite link
f_{ter}	Frequency of terrestrial link
G_{sat}	Gain of the satellite
G_{BS}	Gain of the base station
$G_{dev(HU)}$	Gain of a hybrid user
$G_{dev(PU_{ter})}$	Gain of a primary user requesting service at terrestrial link
$h^x_{s_{arr}}$	Label of hybrid user arrival transitions at the satellite link
$h^x_{t_{arr}}$	Label of hybrid user arrival transitions at the terrestrial link
$h^x_{s_{dept}}$	Label of hybrid user departure transitions at the satellite link
$h^x_{t_{dept}}$	Label of hybrid user departure transitions at the terrestrial link
i^{sat}_{PU}	The number of satellite frequencies used by primary users
i^{ter}_{PU}	The number of terrestrial frequencies used by primary users
i^{ter}_{SU}	The number of terrestrial frequencies used by secondary users
i^{sat}_{HU}	The number of satellite frequencies used by hybrid users retrieving content from the satellite
i^{BS}_{HU}	The number of terrestrial frequencies used by hybrid users retrieving content from the base station
i^{D}_{HU}	The number of terrestrial frequencies used by HUs retrieving content from an HU device
LHS_{PU}	Balance equation left hand side primary user components
LHS_{SU}	Balance equation left hand side secondary user components
LHS_{HU}	Balance equation left hand side hybrid user components

M	The diameter of the area
$N_{f_{sat}}$	Total number of satellite frequencies
$N_{f_{ter}}$	Total number of terrestrial frequencies
N_{HU}	Total number of hybrid user devices
N_0^{sat}	Noise at satellite link
N_0^{ter}	Noise at terrestrial link
p_s^x	Label of primary user transitions at the satellite link
$p_{t_{arr}}^x$	Label of primary user arrival transitions at the terrestrial link
$p_{t_{dept}}^x$	Label of primary user departure transitions at the terrestrial link
P_{sat}^{total}	Total transmission power of satellite
P_{BS}^{total}	Total transmission power of base station
P_{sat}^{ch}	Per channel transmission power of the satellite
P_{BS}^{ch}	Per channel transmission power of the base station
P_{dev}^{tx}	Transmission power of a hybrid user device
$P_{dev}^{rec^{sat}}$	Received power of a hybrid user device from the satellite link
$P_{dev}^{rec^{ter}}$	Received power of a hybrid user device from the terrestrial link
P_{dev}^{idle}	Idling power of a hybrid user device
P_{dev}^{sleep}	Sleeping power of a hybrid user device
P_{BS}^{idle}	Idling power of the base station
P_{BS}^{sleep}	Sleeping power of the base station
$P_{PU_{sat}}^{rec}$	Received power strength of primary user at satellite link
$P_{PU_{ter}}^{rec}$	Received power strength of primary user at terrestrial link
$P_{SU_{ter}}^{rec}$	Received power strength of secondary user at terrestrial link
$P_{HU}^{rec(sat)}$	Received power strength of hybrid user where content is received from satellite
$P_{HU}^{rec(BS)}$	Received power strength of hybrid user where content is received from base station
$P_{HU}^{rec(D)}$	Received power strength of hybrid user where content is received from another hybrid user
$\mathbb{P}_{sat}^{v}$	Probability that a content can be found at satellite
$\mathbb{P}_{BS}^{v}$	Probability that a content can be found at base station

$\mathbb{P}_{dev}^{v}$	Probability that a content can be found at a hybrid device
$\mathbb{P}_{b}^{PU^{sat}}$	Blocking probability of primary users at satellite link
$\mathbb{P}_{b}^{PU^{ter}}$	Blocking probability of primary users at terrestrial link
$\mathbb{P}_{b}^{SU^{ter}}$	Blocking probability of secondary users at terrestrial link
$\mathbb{P}_{b}^{HU}$	Blocking probability of hybrid users
$\mathbb{P}_{d}^{SU^{ter}}$	Dropping probability of secondary users at terrestrial link
$\mathbb{P}_{d}^{HU^{BS}}$	Dropping probability of hybrid users at terrestrial link that retrieve content from the base station
$\mathbb{P}_{d}^{HU^{dev}}$	Dropping probability of hybrid users at terrestrial link that retrieve content from another hybrid user device
r_{sat}	Resource allocation preference ratio for content retrieval from the satellite
r_{BS}	Resource allocation preference ratio for content retrieval from the base station
r_{dev}	Resource allocation preference ratio for content retrieval from a hybrid user device
r_{enh}	The rate of hybrid users that request both base and enhancement contents
$r_{colocated}$	The rate at which base and corresponding enhancement contents are colocated at the same cache
RHS_{PU}^{s}	Balance equation right hand side primary user components at the satellite link
RHS_{PU}^{t}	Balance equation right hand side primary user components at the terrestrial link
RHS_{SU}	Balance equation right hand side secondary user components
RHS_{HU}	Balance equation right hand side hybrid user components
s_{t}^{x}	Label of secondary user transitions at the terrestrial link
s_{zipf}	Zipf distribution parameter
$s(\hat{HU}, v_b)$	Mean base content size requested by a hybrid user
$s(\hat{HU}, v_e)$	Mean enhancement content size requested by a hybrid user
$s(\hat{PU^s}, v_b)$	Mean base content size requested by a primary user at satellite link
$s(\hat{PU^t}, v_b)$	Mean base content size requested by a primary user at terrestrial link

$s(\hat{SU}, v_b)$	Mean base content size requested by a secondary user at terrestrial link
T	Total simulation time
T_{PU}^{sat}	Average service time of primary users at satellite link
T_{PU}^{ter}	Average service time of primary users at terrestrial link
T_{SU}^{ter}	Average service time of secondary users at terrestrial link
T_{HU}^{sat}	Average service time of hybrid users at satellite link that retrieve content from the satellite
T_{HU}^{BS}	Average service time of hybrid users at terrestrial link that retrieve content from the base station
T_{HU}^{dev}	Average service time of hybrid users at terrestrial link that retrieve content from another hybrid user device
$< t_{out}^{dev} >$	The timeout duration for idling period of a hybrid device
$< t_{out}^{BS} >$	The timeout duration for idling period of a hybrid device
Th_{PU}^{sat}	Throughput of primary users at satellite link
Th_{PU}^{ter}	Throughput of primary users at terrestrial link
Th_{SU}^{ter}	Throughput of secondary users at terrestrial link
Th_{HU}^{sat}	Throughput of hybrid users at satellite link that retrieve content from the satellite
Th_{HU}^{BS}	Throughput of hybrid users at terrestrial link that retrieve content from the base station
Th_{HU}^{D}	Throughput of hybrid users at terrestrial link that retrieve content from another hybrid user device
Th_{HU}	Throughput of hybrid users
u	Universal source existance indicator
V	Total number of contents
W_{sat}	Bandwidth of satellite link
W_{ter}	Bandwidth of terrestrial link
λ_{PU}^{sat}	Arrival rate of primary users at satellite link
λ_{PU}^{ter}	Arrival rate of primary users at terrestrial link
λ_{SU}^{ter}	Arrival rate of secondary users at terrestrial link
λ_{HU}	Arrival rate of hybrid users at the system
$\lambda_{PU}^{sat\,*}$	Effective arrival rate of primary users at satellite link

$\lambda_{PU}^{ter\,*}$	Effective arrival rate of primary users at terrestrial link
$\lambda_{SU}^{ter\,*}$	Effective arrival rate of secondary users at terrestrial link
$\lambda_{HU}^{sat\,*}$	Effective arrival rate of hybrid users at satellite link where content is retrieved from the satellite
$\lambda_{HU}^{BS\,*}$	Effective arrival rate of hybrid users at terrestrial link where content is retrieved from the base station
$\lambda_{HU}^{dev\,*}$	Effective arrival rate of hybrid users at terrestrial link where content is retrieved from another hybrid user device
μ_{PU}^{sat}	Service rate of primary users at satellite link
μ_{PU}^{ter}	Service rate of primary users at terrestrial link
μ_{SU}^{ter}	Service rate of secondary users at terrestrial link
μ_{HU}^{sat}	Service rate of hybrid users at satellite link that retrieve content from the satellite
μ_{HU}^{BS}	Service rate of hybrid users at terrestrial link that retrieve content from the base station
μ_{HU}^{D}	Service rate of hybrid users at terrestrial link that retrieve content from another hybrid user device

LIST OF ACRONYMS/ABBREVIATIONS

2D	Two Dimensional
5G	Fifth Generation
AP	Access Point
AVC	Advanced Video Coding
AWGN	Additive White Gaussian Noise
BS	Base Station
CA	Channel Assembling
CDF	Cumulative Distribution Function
CR	Cognitive Radio
CRN	Cognitive Radio Network
CTMC	Continuous Time Markov Chain
D2D	Device to Device
DSA	Dynamic Spectrum Access
DTV	Digital TV
EE	Energy Efficiency
EPB	Energy Per Bit
ESU	Elastic Secondary User
FCFS	First Come First Serve
HAP	High Altitude Platform
HU	Hybrid User
HQ	High Quality
IEEE	Institute of Electrical and Electronics Engineers
ISM	Industrial, Scientific and Medical
LRU	Least Recently Used
MBSC	Multicast Broadcast Service Controller
MoS	Mean Opinion Score
MPEG	Moving Picture Experts Group
MPEP	Maximum Permitted Emission Power

MU-MIMO	Multiple User - Multiple Input Multiple Output
PSNR	Peak Signal to Noise Ratio
PU	Primary User
QoS	Quality of Service
QoE	Quality of Experience
RF	Radio Frequency
RSU	Real-time Secondary User
SVC	Scalable Video Coding
SU	Secondary User
SS	Subscriber Station
TCSA	Two-tier Cooperative Spectrum Allocation
TVWS	TV White Space
UE	User Equipment
WiMAX	Worldwide Interoperability for Microwave Access

1. INTRODUCTION

The mobile broadband explosion propelled with new pervasive services and rich content over Internet is creating an imperative requirement for higher bandwidths and more capacity in wireless networks. To serve this necessity, the radio spectrum is critical in the physical layer. Although it is a limited and valuable resource considering the physical limitations and the burgeoning demand, the utilization of spectrum in various frequency bands in certain areas is shown to be very low [1]. Because of this under-utilization and inefficiency, Cognitive Radio (CR) concept has been proposed and developed in the last decade. In CR paradigm, licensed bands are allowed to be used by a secondary network provided that the secondary network does not affect primary user activities harmfully. It has been touted as a capacity booster for 5G wireless systems [2,3]. Another approach serving higher capacity and improve coverage is to use Device-to-Device (D2D) communications which relies on spatial locality of wireless nodes to offload traffic from the "last-mile" and alleviate the load in the core network while increasing capacity [4]. With D2D operation, mobile devices form direct connections between each other avoiding the routing of data via the radio access network with various benefits such as improved network resource efficiency, lower transmit power and better end-to-end delay [5]. This technique is also integrated into 5G specifications for realizing IMT-2020 vision [6].

On the application side, content consumption oriented services entailing multimedia services (Video-on-Demand and streaming live TV) are emerging as dominant traffic sources. According to Cisco VNI 2015 report, global mobile data traffic grew 69 percent to 2.5 exabytes per month in 2014 [7]. 2014 mobile data traffic was nearly 30 times the size of the entire global Internet in 2000. Moreover, mobile video traffic exceeded 50 percent of total mobile data traffic for the first time in 2012. But such services based on content delivery and transmission have several challenges [8]. For video services, limited bandwidth in wireless systems leads to less fluent flow of images which means degradation in Quality of Experience (QoE) for the users. In case of audio services, for instance voice communications, the delay above a threshold is not

acceptable by the users. Thereof, the transmission of multimedia traffic has to be done with sufficient bandwidth and low delay [9] considering its delay sensitive and bandwidth hungry operation. The solution for how these requirements are to be fulfilled is not trivial. Moreover, advanced encoding techniques such as Scalable Video Coding (SVC) and network layer techniques such as multipath routing render this problem more complex with application and network layer intricacies.

These fundamental research issues in wireless networks are over-arched with one major concern spanning the entire ecosystem, which is energy efficiency (EE). It is fundamental in the sense that it is a "meta-objective" affecting all components/layers of wireless communication systems. The driving factors for EE in wireless systems can be summarized as follows:

- Smaller form-factor devices
- More mobility and more ad hoc settings
- The emergence of green communications concept and environmental issues related to energy consumption and sustainable development
- Operational expenditure reduction via minimization of energy costs
- The widening gap between the development of energy storage capabilities (i.e., batteries) and the advances in circuit design

In this thesis work, we elaborate on layered content transmission over satellite integrated cognitive radio networks (CRNs). The CRN considered is an infrastructure-based system which also utilizes D2D communication mode. A typical layered content example is video content which is scalably-coded such as H.264/Moving Picture Experts Group (MPEG)-4 advanced video coding (AVC). For such situations, throughput has to be improved for better quality of service (QoS) service support while energy consumption is a constraint that has to be under a threshold. Due to energy concerns, wide coverage and control optimization, satellite assistance is a promising enabler. The reason is that satellites of the future will be capable with better coverage and more bandwidth utilizing and with less terrestrial network components, supporting a green network paradigm [10]. The co-existence of satellite and CRNs and moreover their

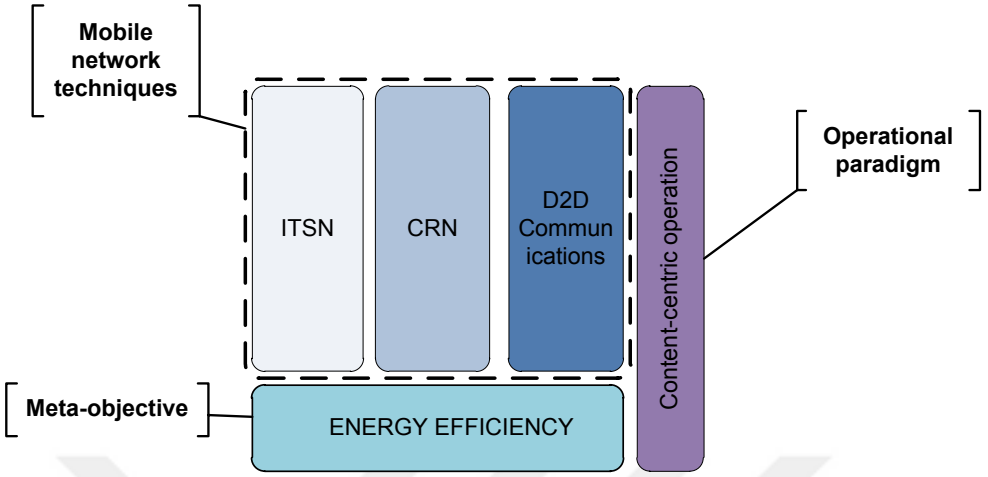


Figure 1.1: The techniques and paradigms integrated and proposed as a system in thesis work. ITSN: integrated terrestrial-satellite network

interpretation is an important research topic [11, 12].

The intersection of layered content delivery and hybrid cognitive networks are yet to be explored comprehensively, especially for the prospective 5G systems [13]. Similarly, satellite systems have been typically studied for conventional wireless systems in niche applications and usually dealing with performance metrics other than energy efficiency (EE). In that regard, the contributions of this thesis are as follows [14]:

(i) We develop an analytical Markovian model for content delivery over satellite integrated cognitive radio networks.

(ii) We devise a simulation for studying this infrastructure-based mobile network. The simulation model is focused on energy efficiency and throughput. However, it can be extended for other performance evaluation purposes.

(iii) We investigate the effect of various system parameters on the performance of these systems. We present multifaceted experimental results on the interplay between different factors such as network density, mode preference, PU traffic activities and average content size in this setting.

Chapter 2 presents related work in the literature. We focus on CRN, hybrid terrestrial/satellite networks, D2D communications and layered content works. In Chapter 3, we present the system model which lays the foundation for our following analytical and simulation-based work. It is a satellite integrated CRN with D2D communications. This system relies on content-centric operation for content delivery function. In the following chapter, we introduce our analysis which is an Markovian analysis for investigating various metrics such as energy-efficiency for this setting. The numerical results are also described in that part. In Chapter 5, the experimental results are discussed for simulation based investigation. Finally, we draw conclusions in Chapter 6 with a perspective on potential research directions.

2. RELATED WORK

The intersection of layered content delivery and hybrid cognitive networks are yet to be explored comprehensively, especially for multi-scale networks (satellite + wide-area cellular + small-area) with D2D operation mode. Although prospective wireless systems, specifically 5G networks, are envisaged to provide content-based and, extremely-low-delay and high-throughput services, the co-existence, and thus utilization, of these concepts are not thoroughly investigated in an integral analysis. There are four main system pillars when such a wireless network is considered:

- cognitive radios for spectral expansion and efficiency
- hybrid satellite and terrestrial network for multi-scale operation
- D2D for proximity-based operation and resource optimization
- layered content at the application layer

Nevertheless, there is large body of literature focusing on a single aspect (e.g. CRNs) or tuple of them (e.g. cognitive satellite networks). In this section, we venture to provide a concise yet comprehensive survey of such works.

There is a plethora of work on CRN, especially for core issues such as resource allocation or mobility regarding various emerging aspects such as green communications, heterogeneous settings and for applications such as multimedia traffic [15, 16]. In [17], a channel allocation model for multimedia transmission across infrastructure based CRNs is proposed. Markov chain model is constructed for centralized CRN that contains access points (APs) and user equipments (UEs) with multiple antennas. AP is the central entity for channel allocation. Jiang et al. consider three communication modes where communication can be within centralized CRN, from outside of centralized CRN to a node of the centralized CRN and from a node of centralized CRN to outside of centralized CRN. All possible arrival and departure of each communication mode and arrival and departure of primary user causes a transition in the state diagram. The authors have done both analysis and simulations for the proposed method.

In general, the simulation results are consistent with analytical results. The metrics they have used are blocking probability, dropping probability and throughput. In the first simulation, Jiang et al. consider primary users (PUs) and two different type of multimedia streaming secondary users (SUs) having different type of communication modes. The outcomes are as follows: With increasing arrival rate of PUs, the blocking probability of PUs and dropping probability of both types of SUs increase but throughput of both types of SUs decrease. In the next simulation setting, they consider PUs and nine different streaming SUs. They observe that with increasing arrival rate of PUs, the blocking probability of PUs and dropping probability of all types of SUs increase whereas throughput of all types of SU types decrease.

Smart grid applications have certain QoS requirements such as low latency and high reliability. Due to the high amount of data transmission in smart grids, higher spectrum utilization by using CR systems is a promising solution. Wireless multimedia sensor and actor networks can be used in smart grids to perform good QoE requirements. In [18], Wang et al. study challenges of and solutions to CRN with multimedia communication for smart grids. In their model, they assume that different traffic types exist in the system. The traffic with the highest priority is the power schedule information. Smart meter data have lower priority and the data from environment monitoring has even lower priority. The channel allocation should be done taking the traffic type and corresponding QoE into account. The channel allocation is modeled as a two dimensional (2D) Markov model containing two types of users, namely PU and SU. They assume that there are k types of SUs with different priorities. According to their simulation results, at a given SU arrival rate the peak signal to noise ratio (PSNR) decreases with decreasing priority. Also, it is shown that with increasing arrival rate of SUs, PSNR decreases. These results show how the multimedia quality is affected by arrival rates. They consider a cognitive channel allocation scheme for power scheduling of the grid while taking QoE of users into account. As frequency switching increases transmission delay, the proposed framework allocates delay-sensitive data to bands with lower switching probability.

In [19], Park et al. propose a system using Multiple User - Multiple Input Multiple Output (MU-MIMO) and SVC coded video streams. They want to maximize the sum utility taking QoE into account in case of restricted power and bandwidth. As this problem is not easy to solve they use approximate correction rate, thus making the problem convex. They try to find the best modulation possible to find optimal power and rate. The proposed method has better sum-utility, higher number of layers transmitted properly and higher PSNR and structure similarity values when compared to a baseline water-filling algorithm.

In [20], power allocation problem in cognitive satellite terrestrial networks are investigated. The satellite network is assumed to be a primary network whereas the terrestrial network is the secondary network. The resource allocation problem is defined as follows: Maximizing the effective rate of the terrestrial link (secondary link) according to a given QoS requirements (parameter θ) while keeping the outage probability of the satellite link under a Q_{out} value. The resource allocation problem is investigated both under perfect channel estimation and imperfect channel estimation. According to their simulations they derive the following results: By allowing higher unsuccessful transmission probability of satellite link due to interference from base station (BS), the effective capacity of the terrestrial link is increased. For tighter QoS requirements of secondary link, the effective capacity of secondary link is decreased. With less shadowing on satellite links, the effective capacity of secondary link decreases. However, with lower fading in the secondary link, the effective capacity of the secondary link increases. With lower fading in the interfering link from BS to satellite user, the effective capacity of the secondary link decreases. In general, with increasing estimation error variance, additional unsuccessful transmission probability of satellite link increases.

In [21], Kawamoto et al. study an effective context-aware service (content) delivery across cooperative satellite-terrestrial networks. They construct a cooperative satellite/terrestrial model which consists of satellite cells and terrestrial cells. They propose a context-aware bandwidth allocation scheme to maximize the number of users provided with context-aware contents. Initially, they determine the allocation of the bandwidth for each satellite cell by making use of satellite's broadcasting/multicasting

nature. Next, they try to find the optimal allocation for satellite and terrestrial network resources to maximize the number of users reaching the context-aware contents. When many users need to access the same content, it is preferable to use satellite link for multicasting/broadcasting. When a user needs to access a context-aware content individually, terrestrial link is preferable. According to the calculations for the number of users reaching context-aware content with the same number of multicast contents in satellite-only, terrestrial-only and their proposed model, the proposal has the highest number of users reaching content.

In [22], Ge et al. propose two-tier cooperative spectrum allocation (TCSA) method for multimedia transmission over CRN. This method takes QoS requirements of SUs into account and tries to optimize the spectrum handoff rate of SUs and the spectrum utilization. According to the quality of spectrum regions and SUs' needs, the order of available spectrum regions are ranked by a spectrum adjacency algorithm. This algorithm is used for meeting the QoS requirements of SUs for various multimedia applications. Besides, a max hyper-weight matching algorithm is used to optimize the spectrum handoff rate of SUs and the spectrum utilization jointly. In the simulations they consider voice, video and data transmissions. As spectrum regions, they use industrial, scientific and medical (ISM) and cellular bands. They show that TCSA prefers cellular bands for voice and mostly ISM bands for video and data. They compare proposed TCSA method with cost-minimized and random matching algorithms both for throughput and handoff rate. TCSA has the highest throughput of all three methods and it has the lowest handoff rate of all methods for any number of SUs in the system.

In [23], Jiang et al. propose a channel allocation method where the primary channels are not homogeneous and different QoE requirements of SUs are taken into account for the channel allocation. They construct a priority queue for SUs. The SUs requiring lower delay are assigned with high priorities whereas SUs that are delay tolerant have low priorities. They compare the priority system with the setting without priority for blocking probability, dropping probability and throughput. In priority systems, high priority users get higher throughput and lower dropping probability compared to non

priority systems. With the increasing idle probability of primary channel, mean PSNR increases for all types of SUs. High priority SUs have higher mean PSNR values than low priority SUs in general for any given primary channel idle probability. With the increasing arrival rate of SUs, mean PSNR decreases for all types of SUs. Again, high priority SUs have higher mean PSNR than low priority SUs in general for any given arrival rate of SUs. They test multimedia quality with three videos, namely Akiyo, Carphone and mother and daughter. For the video Akiyo, it is shown that by increasing idle probability of primary channel, mean PSNR for all types of SUs increases. High priority SUs have higher mean PSNR than low priority SUs. With increasing dropping probability, Mean Opinion Score (MoS) value for QoE decreases. When compared with non-priority system, priority system has lower dropping probability range together with higher MoS values.

In [12], Bayhan et al. present a novel concept, namely high altitude platform (HAP) driven smart radios, where CR devices are dynamically configured and policies for dynamic spectrum access are beamed with the assistance of a HAP and a back end satellite subsystem. They provide some simulations where some primary IEEE 802.11b/g users communicate in infrastructure mode through three base stations while some SUs having different priorities for the available spectrum communicate opportunistically.

In [24], a centralized dynamic spectrum access (DSA) for CRNs with three user types, namely PU, high priority SU and low priority SU, is proposed. PUs have high priority over all types of SUs. High priority SUs have priority for channel access and handoff over low priority SUs. A PU can be assigned to one channel that consists of N subchannels whereas a high priority SU can be assigned to N_1 subchannels and a low priority SU can be assigned to N_2 subchannels. They model the system with Markov chains where the state holds number of users for each type. From the state diagram using the balance equations, the steady state probabilities are derived for each state. The blocking and dropping probabilities are derived using steady state probabilities for high and low priority SUs. With the increasing arrival rate of PU users, blocking and dropping probabilities of high and low priority SUs increase. The blocking and

dropping probabilities of high priority SUs is less than low priority SUs for the same set of parameter values due to higher priority. By increasing the number of channels and subchannels, blocking and dropping probabilities can be reduced for any type of SU.

In [25], queue based dynamic channel assembling (CA) method is proposed for CRNs with three types of users namely PUs, elastic SUs (ESUs) and real-time SUs (RSUs). The system contains one queue devoted for ESUs and another queue for RSUs. In the dynamic channel access strategy, an ESU can have at least W and at most V channels but an RSU can have fixed number of channels for service. Two different queueing schemes are proposed. The terminated ESUs are not fed back to the queue devoted for ESUs in the first scheme, whereas the interrupted ESUs are fed back unless the queue is full in the second scheme. In each scheme, both queues operate with First-Come-First-Serve (FCFS) principle. The priority level of the queue devoted for RSUs is higher than the queue devoted for ESUs. For the performance analysis, Continuous Time Markov Chains (CTMCs) are constructed. From the state diagram using the balance equations, the steady state probabilities are derived for each state. By using steady state probabilities, secondary network capacity of ESU and RSU services, spectrum utilization, blocking probability of ESU and RSU services, average PU interruption rate of ESUs, forced termination probability of ESU and RSU services, mean queue length and finally average total delay of SU services are derived for each queuing scheme.

With increasing arrival rate of ESU, the capacity of ESU services and spectrum utilization increase. At a fixed arrival rate of ESU, queued systems have higher capacity of ESU services and spectrum utilization. With increasing the queue size given other parameters fixed, both capacity of ESU services and spectrum utilization increase. Additionally, second queueing scheme performs better than first queueing scheme in terms of capacity and spectrum utilization. With increasing PU service rate, blocking probability of ESU decreases and forced termination probability of ESU services increases. At a fixed PU service rate, queued systems have lower blocking probability of ESU. When the queue size is increased with other parameters fixed, blocking probability of

ESU decreases. Second queueing scheme performs worse than first queueing scheme in terms of blocking probability of ESU. Moreover, the average total delay of ESU services is higher in the second queueing scheme. However, second one performs better than first one in terms of forced termination probability of ESU services due to feedback mechanism of the second scheme. The average total delay of RSU services is almost equal in both queueing schemes. RSU services have less delay than ESU services. For a required level of QoS, the maximum possible ESU arrival rate can be found by using the results for blocking, forced termination probabilities of ESU and average total delay and choosing the rate accordingly.

In [26], DSA methods for CRNs with three types of users namely PU, high priority SU and low priority SU is investigated. A PU can be assigned to one channel that consists N subchannels whereas any SU can be assigned to one subchannel only. DSA methods are mainly divided into two groups: centralized and distributed. Four different centralized DSA methods (CDSA-I to IV) and two different distributed DSA methods are proposed. In all methods, two different priority classes for SUs are considered and a number of subchannels are reserved for high priority SUs. All of these methods differ in terms of handoff mechanisms. In CDSA-I, when a PU arrives, if there is no idle subchannel SUs are displaced and high priority SUs can be assigned to subchannels of low priority SUs. No such displacement of high priority SUs to low priority SUs is allowed in CDSA-II. CDSA-III and CDSA-IV are the buffered versions of CDSA-I and CDSA-II methods, respectively. In all distributed DSA methods, displaced SUs upon the arrival of PUs contend for idle subchannels. In the first distributed DSA method, the displaced SUs that cannot be handed-off are terminated. In the second distributed DSA method the displaced SUs are kept at a virtual buffer to allow them to contend for subchannels in next slots instead of being terminated.

For the performance analysis CTMCs of each DSA are constructed. The blocking probabilities, forced termination probabilities, call completion rates and mean handoff delay are derived using steady state probabilities for high priority SUs and low priority SUs for all DSA methods. DSA methods with handoff buffer have higher call completion rates compared to non-buffered DSA methods. CDSA-I has higher call completion

rate of high priority SUs compared to CDSA-II. Additionally, the forced termination probability for high priority SUs of CDSA-I is lower than that of CDSA-II. Both of these results are due to the displacement mechanism of high priority SUs to low priority SUs in case of no idle subchannel. With increasing PU arrival rate, handoff delays of both high and low priority SUs increase. Distributed DSA schemes experience the highest handoff delays for both high and low priority SUs. CDSA-III has the lowest handoff delay of high priority SUs since high priority SUs can replace low priority SUs. CDSA-IV has the lowest handoff delay of low priority SUs. The reason is that high priority SUs can not displace low priority SUs in that scheme. In general, buffer increases call completion rate while handoff delay appears.

In [27], Gur et al. describe and discuss a heterogeneous system of satellite and IEEE 802.16 Worldwide Interoperability for Microwave Access (WiMAX) networks collaborating for the efficient delivery of multimedia services. They elaborate on the rationale behind integrated satellite and WiMAX networks and propose a diverse set of enhancements and additions into WiMAX BS and Multicast Broadcast Service Controller (MBSC), which allows this interworking in the multimedia delivery context. They also describe a WiMAX BS downlink scheduler that considers satellite channel conditions of the dual-mode Subscriber Stations (SSs) while making resource allocation and packet scheduling. This scheduler interacts with another proposed module in MBSC, namely Satellite-Terrestrial Interaction Module, for performing these operations. Traffic for real-time multimedia and cache-based delivery is considered in the system. On the SS side, a lightweight signaling scheme between BS and SS for service continuity and control is presented. However, their scheme lacks the CR and D2D dimensions and solely focuses on hybrid network operation.

For facilitating content downloading and consumption, D2D communication is instrumental to increase the spectral efficiency and to enhance the system capacity. In [28], Li et al. investigate the fundamental problems of how D2D communication improves the system performance of cellular networks and what the potential effect of D2D communication is. They develop optimal solutions for resource allocation and mode selection problems under realistic user and mobility conditions. They obtain the

theoretical upper bound to system content-downloading performance via a max-flow optimization problem. Utilization of vacant spectrum rather than underlay operation for D2D communications is also an important research topic. In [29], Ding et al. presents a crowd-sensing based approach to exploit TV white space (TVWS) for D2D communications with the aid of the existing cellular infrastructure. Their goal is to build a location-specific TVWS database, which provides a look-up table service for any D2D link to determine its maximum permitted emission power (MPEP) in an unlicensed digital TV (DTV) band. They develop a powerful fixed point continuation algorithm to reconstruct the unknown elements from the known elements regarding incomplete sensing data. Moreover, an opportunistic spatial reuse algorithm is developed for each D2D link to determine its MPEP.

There are also game-theoretic approaches for resource sharing and optimization issues in D2D communications. In [30], Chen et al. consider the problem of resource sharing in D2D communication underlaying cellular networks. The problem is formulated as a non-cooperative game in which mobile users decide their respective transmission power over available resource blocks (RBs) with the goal of maximizing their own utility function. They propose a novel design of the utility function which is defined for each user as the achievable rate normalized by the power consumption. The most energy efficient strategy turns out that a D2D UE allocates the least amount of power on the channel with the best channel gain-to-interference-plus-noise-ratio (CINR) yet still achieves the highest data rate on that channel while a cellular UE allocates the optimal power on its assigned channel to reach the maximum energy efficiency.

In conclusion, the literature lacks comprehensive treatment of hybrid networks with terrestrial segments employing CR capability and D2D operation and honed for content-centric operation. Although it is a challenging research issue, the investigation of such systems is paramount considering the open problems related to resource efficiency, content delivery and QoE in next-generation mobile networks.

3. CONTENT-ORIENTED SATELLITE INTEGRATED COGNITIVE RADIO NETWORK

In this chapter, we describe our concept of content-oriented satellite integrated CRN. Although there are different endeavors to model/analyze such heterogeneous wireless systems, it is not evident how to attain such a goal for this complex and multi-dimensional structure [31]. We construct our model progressively considering the practicality and tractability. In the following chapters, this model is further refined.

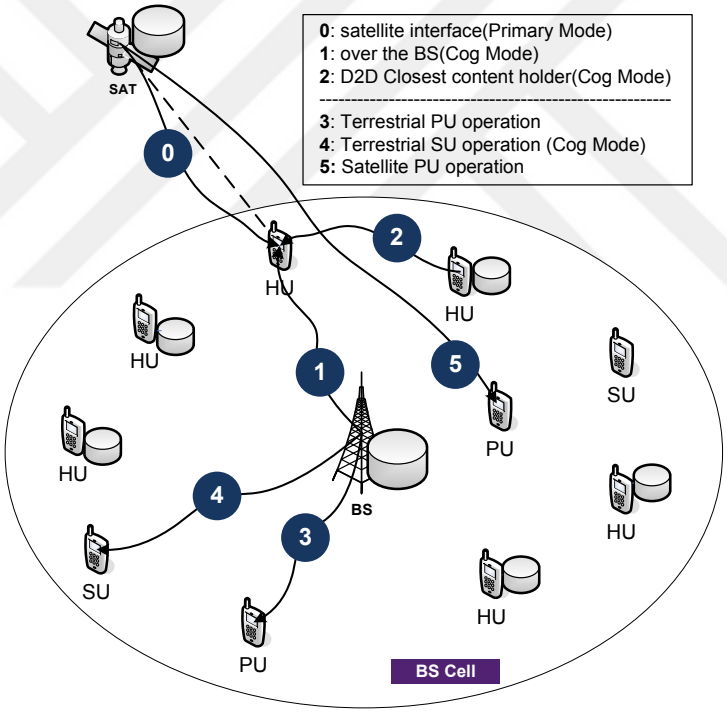


Figure 3.1: System model. There are different operation modes based on the attached entity (satellite, BS, other device).

First, let us briefly introduce the network structure. There is one satellite, one BS, PUs, SUs and hybrid users (HUs) and we investigate the area of the BS cell as shown in Figure 3.1. The network is composed of two links, namely satellite and terrestrial. The standard PU and SU operations are shown with labels 3, 4 and 5 in Figure 3.1. In this network we mainly focus on the HUs. When they retrieve content from the

satellite as shown by the label 0 in Figure 3.1, they are in PU mode. When they retrieve content through the terrestrial frequencies either from the BS or from some HU device via D2D communication shown by labels 1 and 2 respectively, they are in SU mode. When a PU appears during the content retrieval, it preempts the terrestrial frequency immediately. The purpose of such a network is to transmit contents with better throughput and energy efficiency.

The key assumption is that we consider a receiver-driven chunk-based content-oriented system where the content is stored and identified as uniquely identifiable chunks (segments) [32]. These chunks are transported at chunk level with built-in network storage for caching. We do not make any assumptions on specific naming or content-based routing mechanisms employed in content-oriented operation [33]. We assume necessary mechanisms are already employed in the network nodes.

We focus on multimedia content retrieval in our system. HUs may request standard quality or high quality contents. To enable flexibility, layered content structure is used. Each content has base and enhancement parts as shown in Figure 3.2. Detailed information is given in Chapter 5.

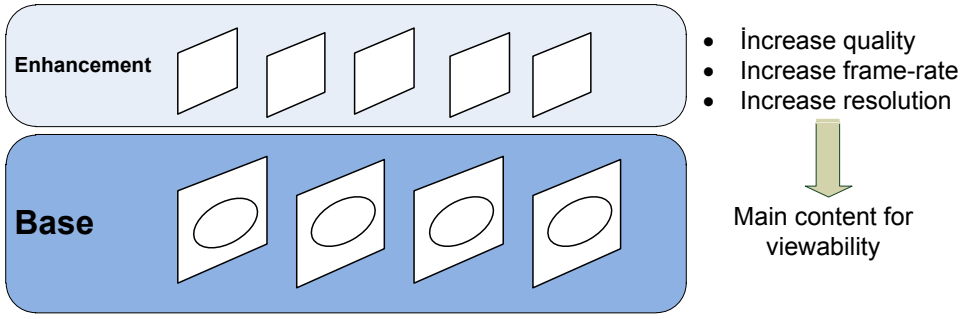


Figure 3.2: Layered content abstraction entailing base and enhancement layers.

This network relies on on four main premises for achieving higher capacity with higher efficiency as noted in Chapter 1, which are

- Cognitive radios for spectral efficiency: Dynamic spectrum access provides better spectral efficiency converging to the full utilization of frequency resources [34].
- Hybrid satellite and terrestrial network for multi-scale operation: The coverage scale for satellite networks are much larger compared to macro or small cells. They provide wider coverage and utilize solar power to operate [35].
- D2D for proximity-based operation and resource optimization: The D2D content transmission improves frequency reuse and exploits the physical layer advantages and lower power consumption due to proximity.
- Layered content at the application layer: The layered coding of multimedia content provides multi-quality content transmission and representation according to network and device conditions [36].

Rendering these fundamental elements, in the following chapters we investigate this system analytically and experimentally (using simulations) in different settings and provide insight into performance focusing on key metrics such as energy efficiency.

4. ANALYTICAL SYSTEM MODEL

In this chapter, we develop an analysis of the system in question using Markovian analysis. Our motivation is to analyze satellite integrated cognitive radio networks for energy efficiency when content dissemination for mobile devices is the primary use-case.

For providing mobile content delivery with longer battery lifetime and smaller form-factor devices, and minimizing environmental and operational costs, we need to attain energy efficiency in our network, i.e. minimize the energy consumption per successfully transmitted content bits.

4.1. System Model

In our system model, we assume that there are two main segments in our network, namely satellite and terrestrial. The frequencies that are used by satellite and terrestrial parts are mutually exclusive. We assume that there is one satellite at frequency level f_{sat} with bandwidth W_{sat} while the terrestrial system is at frequency level f_{ter} with bandwidth W_{ter}. In the analyzed topology, there is one cell covered by a BS although the analysis can be extended for larger multi-cell topologies.

On the user side, there are some users that have cognitive abilities and some that do not have such abilities (PUs). The users with no cognitive abilities and no opportunistic channel access are PUs while SUs can operate "cognitively" and access the medium opportunistically. Satellite frequencies cannot be accessed opportunistically and are solely dedicated to satellite operation.

In our model, there are three types of users:

(i) PUs that can be served over satellite or terrestrial frequencies by satellite or BS, respectively.
(ii) SUs that can opportunistically access the terrestrial frequencies. They are served

by the BS.

(iii) HUs that can be in one of two modes: SU or PU operation. We mainly focus on this user type since they facilitate the promise of the system for higher efficiency via cognitive and D2D expansion. When they are in PU mode, they can be served by satellite frequencies over the satellite. When they are in SU mode, they can opportunistically access terrestrial frequencies that are served by either terrestrial BS or another content holder HU. PU mode operating at satellite frequencies is useful for the additional frequency introduction apart from the terrestrial frequencies whereas SU mode is useful due to spectral efficiency and D2D operation with lower power consumption. The mode selection is done according to a preference configuration, satellite channel state and terrestrial channel state that is to be explained in Section 4.6.3.

We assume that our system has no control over baseline PUs and SUs. Our system has a priori knowledge about PU traffic, SU traffic and HU traffic models. Although this is a strong assumption, it can be realized via central sensing and monitoring capabilities of BS. The resource allocation is done centrally by the BS. It allocates resources to HUs taking frequency state into account. That is, the central entity can detect PU and SU arrivals and departures without failure and it can allocate resources to HUs knowing the PU and SU activities. We do not focus on the sensing errors since our main goal is to analyze potential performance improvement in a such an integrated sytem. The signaling operation/overhead from BS to satellite and HU devices are ignored for the sake of brevity.

4.2. Content Model

In this section, we describe the content model and content availability in the network. A content is assumed to be a self-contained chunk of video. An entire content is assumed to be at the same place, i.e. it is not allowed that some portion is in the satellite and the rest in an HU device. This is related to the fundamental property of being "self-contained". For each content holder (satellite, BS or an HU device), a probability of content availability is assigned. For instance, $\mathbb{P}^{v}_{sat} = 0.5$ means that a

content can be found at the satellite with probability 0.5.

For tractability, we ignore base and enhancement content differentiation in our analytical course and assume all contents are of base type. It is integrated into simulation based investigation described in Chapter 5. Contents are uniformly assumed to be base type. We also assume that all contents have identical popularity i.e. popularity distribution is not employed in the analysis. This approach is adopted since we aim to provide a general analytical model such that the outcome of analysis is expected to be independent of popularity distribution.

4.3. Traffic Model

The video request of any user type corresponds to an arrival for the system service. The video service given to a user type is named as departure. The arrival of any type of users is Poisson. The service to any user type is exponentially distributed. Our system is modeled with CTMC. To be able to satisfy the markov property, that is the state transitions depends only on the current state not the previous states, HU data retrieval from a content holder is not changed in case of PU interruption. That is, HU does not continue content retrieval from another content holder. HU continues content retrieval from the same content holder via an idle channel. If no idle channel exists, it is dropped. The system has no buffer for dropped requests for future service retrials. PUs have priority over other SUs or HUs in SU mode. Due to priority of PU preemption is allowed. When the system is full and a new user PU comes, a user with low priority will be discarded. No overlay is allowed. One frequency can be used by only one user at a time.

4.4. Assumptions and Parameters

For the analytical analysis, we consider non-time slotted scheme. We ignore transmission, sensing errors and waiting times for the sake of simplicity. We consider the region of a BS. We assume that all the regions have the same arrival and service rates for each user type. Therefore, concentrating on one of the regions does not result

in the loss of generality.

The parameters for analitical analysis are given at Table 4.1 and Table 4.2.

Table 4.1: Analytical parameters.

Parameter	**Value**	**Explanation**
$N_{f_{sat}}$	3	Total number of satellite frequencies
$N_{f_{ter}}$	5	Total number of terrestrial frequencies
λ_{PU}^{sat}	0.09 $\frac{user}{sec}$	Arrival rate of primary users at satellite link
λ_{PU}^{ter}	0.25 $\frac{user}{sec}$	Arrival rate of primary users at terrestrial link
λ_{SU}^{ter}	0.25 $\frac{user}{sec}$	Arrival rate of secondary users at terrestrial link
λ_{HU}	0.16 $\frac{user}{sec}$	Arrival rate of hybrid users at the system
P_{sat}^{total}	144 W	Total transmission power of satellite
P_{BS}^{total}	30 W	Total transmission power of base station
P_{sat}^{ch}	48 W	Per channel transmission power of the satellite
P_{BS}^{ch}	6 W	Per channel transmission power of the base station
P_{dev}^{tx}	80 mW	Transmission power of a hybrid user device
d_{sat}	300 km	Distance from satellite to earth
d_{BS}	$\frac{300}{2}$ m	Mean distance to the base station of a primary user, secondary user and/or hybrid user
d_{D2D}	50 m	Mean distance between receiver and sender hybrid user devices

Table 4.2: Analytical parameters.

Parameter	**Value**	**Explanation**
W_{ter}	2 MHz	Bandwidth of terrestrial link
W_{sat}	36 MHz	Bandwidth of satellite link
f_{sat}	20 GHz	Frequency of satelite link
f_{ter}	700 MHz	Frequency of terrestrial link
G_{sat}	$2.5 \cdot 10^4$	Gain of the satellite
G_{BS}	$4 \cdot 10^{-5}$	Gain of the base station
$G_{dev(HU)}$	$6 \cdot 10^{-2}$	Gain of a hybrid user
$G_{dev(PU_{ter})}$	$11 \cdot 10^{-2}$	Gain of a primary user requesting service at terrestrial link
N_0^{sat}	$1e^{-18}\frac{Watt}{Hz}$	Noise at satellite link
N_0^{ter}	$1.585e^{-19}\frac{Watt}{Hz}$	Noise at terrestrial link
$s(\hat{PU^s}, v_b)$	25 Mbits	Mean base content size requested by a primary user at satellite link
$s(\hat{PU^t}, v_b)$	25 Mbits	Mean base content size requested by a primary user at terrestrial link
$s(\hat{SU}, v_b)$	25 Mbits	Mean base content size requested by a secondary user at terrestrial link
$s(\hat{HU}, v_b)$	25 Mbits	Mean base content size requested by a hybrid user

The Friis transmission equation for PU, SU and HU content retrievals from the satellite, the BS and HU device are shown below in equations 4.1, 4.2, 4.3, 4.4, 4.5 and 4.6, respectively. Using these equations and parameter values, we can calculate

received power P in Watts.

$$P^{rec}_{PU_{sat}} := \frac{P^{ch}_{sat} \times G_{sat} \times G^{D}_{r} \times c^2}{(4\pi \times f_{sat} \times d_{sat})^2} \tag{4.1}$$

$$P^{rec}_{PU_{ter}} := \frac{P^{ch}_{BS} \times G_{BS} \times G_{dev(PU_{ter})} \times c^2}{(4\pi \times f_{ter} \times d_{BS})^2} \tag{4.2}$$

$$P^{rec}_{SU_{ter}} := \frac{P^{ch}_{BS} \times G_{BS} \times G^{D}_{r} \times c^2}{(4\pi \times f_{ter} \times d_{BS})^2} \tag{4.3}$$

$$P^{rec(sat)}_{HU} := \frac{P^{ch}_{sat} \times G_{sat} \times G_{dev(HU)} \times c^2}{(4\pi \times f_{sat} \times d_{sat})^2} \tag{4.4}$$

$$P^{rec(BS)}_{HU} := \frac{P^{ch}_{BS} \times G_{BS} \times G_{dev(HU)} \times c^2}{(4\pi \times f_{ter} \times d_{BS})^2} \tag{4.5}$$

$$P^{rec(D)}_{HU} := \frac{P^{tx}_{dev} \times G_{dev(HU)} \times G_{dev(HU)} \times c^2}{(4\pi \times f_{ter} \times d_{D2D})^2} \tag{4.6}$$

Since we do not want to distinguish among higher and lower frequencies in terms of capacity, our analytical investigation does not track which frequency is used by which user at each instant of time and we use the mean transmission frequency value for each case during calculations. The frequency dispersion around the respective mean values is very small and thus such simplification does not affect the results in a discernible way.

The Shannon capacities under Additive White Gaussian Noise (AWGN) are shown below. Using these formulae, we calculate the channel capacities for content retrieval in bits per second.

$$C^{x}_{PU} := W_x log_2(1 + (\frac{P^{rec}_{PU_x}}{N^{x}_{0} \times W_x})) \text{ where } x \in \{sat, ter\} \tag{4.7}$$

$$C^{ter}_{SU} := W_{ter} \times log_2(1 + (\frac{P^{rec}_{SU_{ter}}}{N^{ter}_{0} \times W_{ter}})) \tag{4.8}$$

$$C^{sat}_{HU} := W_{sat} \times log_2(1 + (\frac{P^{rec(sat)}_{HU}}{N^{sat}_{0} \times W_{sat}})) \tag{4.9}$$

$$C^{x}_{HU} := W_{ter} \times log_2(1 + (\frac{P^{rec(x)}_{HU}}{N^{ter}_{0} \times W_{ter}})) \text{ where } x \in \{BS, D\} \tag{4.10}$$

By dividing the channel capacities by average content size, we get the service rates μs

of different user types.

$$\mu_{PU}^{x} := \frac{C_{PU}^{x}}{s(\hat{PU^{s}}, v_b)} \text{ where } x \in \{sat, ter\} \tag{4.11}$$

$$\mu_{SU}^{ter} := \frac{C_{SU}^{ter}}{s(\hat{SU}, v_b)} \tag{4.12}$$

$$\mu_{HU}^{x} := \frac{C_{HU}^{x}}{s(\hat{HU}, v_b)} \text{ where } x \in \{sat, BS, D\} \tag{4.13}$$

which are used for the analytical model.

4.5. State Diagram

The state in our model represents the number of satellite frequencies used by PUs, the number of terrestrial frequencies used by PUs, the number of terrestrial frequencies used by SUs, the number of satellite frequencies used by HUs, the number of terrestrial frequencies used by HUs retrieving content from the BS and the number of terrestrial frequencies used by HUs retrieving content from an HU device.

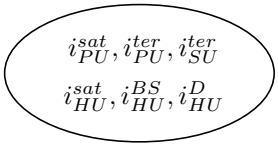


Figure 4.1: State.

The system does not get into a state and become stuck there. For reaching a state, there is always a path starting from the initial state and by each arrival of PU, SU and/or HU reaching the state with the corresponding number of users active at corresponding frequencies. Since the service durations are finite, the departure rates are finite which implies that there is a path for departure for each type of user. Hence, the system does not get stuck in some state.

The number of idle frequencies can be calculated according to the state components. The function $idle^{sat}(x)$ is defined to be the number of idle frequencies at the satellite link at some state x and $idle^{ter}(x)$ is defined to be the number of idle

frequencies at terrestrial link at state x.

$$idle^{sat}(x) := N_{f_{sat}} - i^{sat}_{PU}(x) - i^{sat}_{HU}(x) \tag{4.14}$$

$$idle^{ter}(x) := N_{f_{ter}} - i^{ter}_{PU}(x) - i^{ter}_{SU}(x) - i^{BS}_{HU}(x) - i^{D}_{HU}(x) \tag{4.15}$$

$$1_{(\theta)} := \begin{cases} 1, & \text{if } \theta \text{ is true} \\ 0, & \text{otherwise.} \end{cases} \tag{4.16}$$

Note that Equation 4.16 is used in state transitions.

4.6. State Transitions

To establish our model, we also describe state transitions in the system. A state transition can be triggered by one of six different events, namely a PU arrival, a PU departure, an SU arrival, an SU departure, an HU arrival and an HU departure.

4.6.1. PU Transitions

First let us investigate how the system changes due to PU service requests and completions at the satellite link. Assume that State 1 in Figure 4.2 is a valid state.

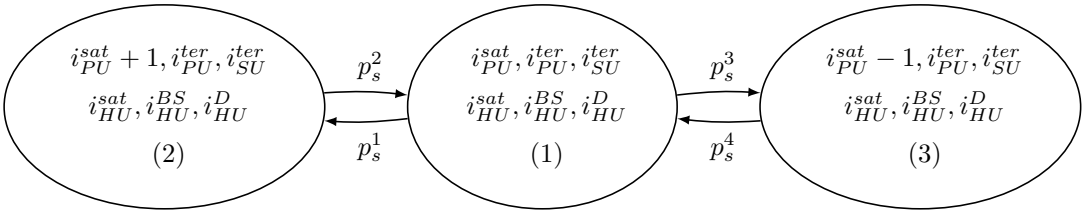


Figure 4.2: PU transitions at the satellite link.

PU transitions at the satellite link are labeled with p^x_s where $x \in \{1, 2, 3, 4\}$. The corresponding values are shown in the Table 4.3 with the corresponding type. At the satellite link, only PUs and HUs in PU mode can be active. Therefore, PUs can arrive to the satellite link only when there are idle satellite frequencies in the system which can be seen at p^1_s and p^4_s transition label values. Since no SU is active at the satellite

link in our system model, no preemption occurs.

Table 4.3: PU transitions at the satellite link.

Variable	**Value**	**Type**
p_s^1	$\lambda_{PU}^{sat} 1_{(idle^{sat}(1)>0)}$	Arrival
p_s^2	$(i_{PU}^{sat}(1)+1)\mu_{PU}^{sat} 1_{(idle^{sat}(1)>0)}$	Departure
p_s^3	$i_{PU}^{sat}(1)\mu_{PU}^{sat}$	Departure
p_s^4	$\lambda_{PU}^{sat} 1_{((idle^{sat}(3)>0)\wedge(i_{PU}^{sat}(1)>0))}$	Arrival

Now let us investigate how the system changes due to PU service requests and completions at the terrestrial link. Assume that State 1 in Figure 4.3 is a valid state.

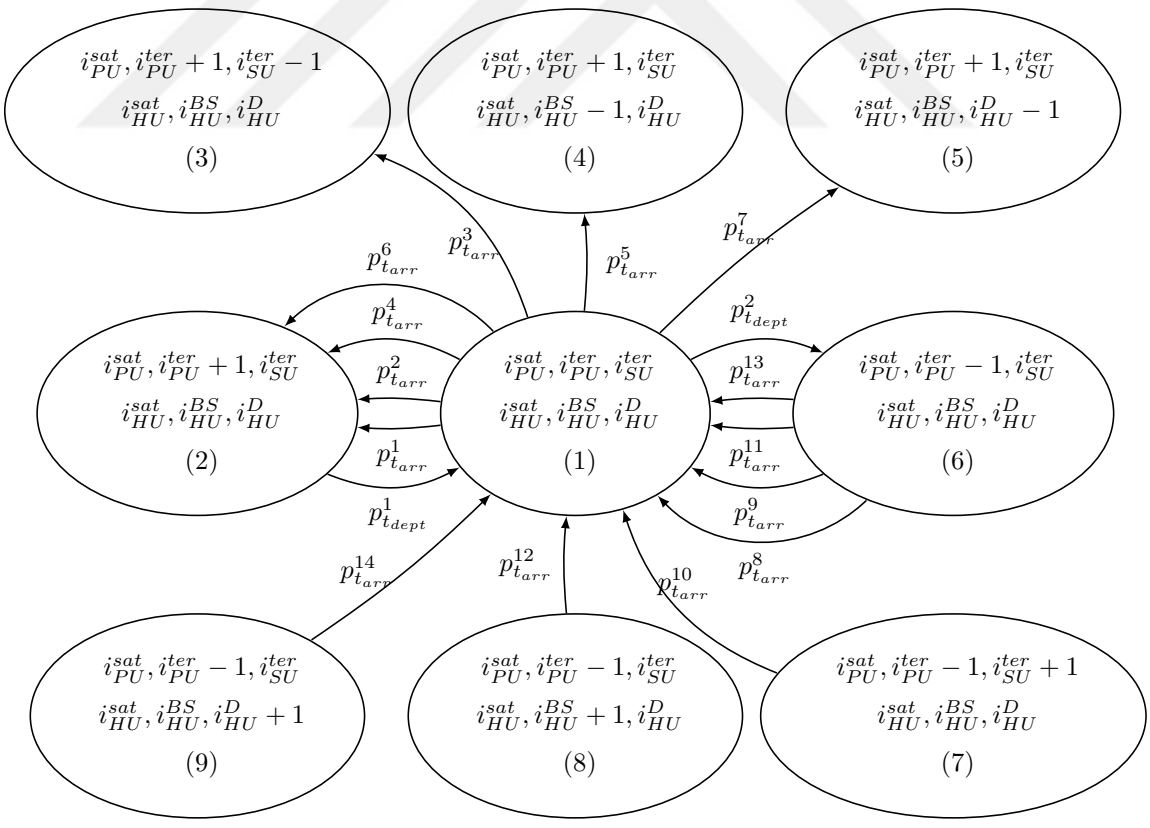


Figure 4.3: PU transitions at the terrestrial link.

PU arrival transitions at the terrestrial link are labeled with $p_{t_{arr}}^x$ where $x \in \{1, 2, ..., 14\}$ and PU departure transitions at the terrestrial link are labeled with $p_{t_{dept}}^x$

where $x \in \{1, 2\}$. The corresponding transition values are shown in Table 4.4. $p^1_{t_{arr}}$ and $p^8_{t_{arr}}$ are the labels of the transitions where PU arrives to an idle frequency. $p^2_{t_{arr}}$ and $p^9_{t_{arr}}$ are the labels of the transitions where PU arrives at an SU occupied frequency and SU is moved to an idle channel. $p^3_{t_{arr}}$ and $p^{10}_{t_{arr}}$ are the labels of the transitions where PU arrives at an SU occupied frequency and SU is dropped due to the lack of idle frequency at the terrestrial link. $p^4_{t_{arr}}$ and $p^{11}_{t_{arr}}$ are the labels of the transitions where PU arrives at an HU occupied frequency retrieving content from the BS and HU is moved to an idle channel. $p^5_{t_{arr}}$ and $p^{12}_{t_{arr}}$ are the labels of the transitions where PU arrives at an HU occupied frequency retrieving content from the BS and HU is dropped due to the lack of idle frequency at the terrestrial link.

Table 4.4: PU transitions at the terrestrial link.

Variable	**Value**
$p^1_{t_{arr}}$	$\lambda^{ter}_{PU} \frac{idle^{ter}(1)}{N_{f_{ter}} - i^{ter}_{PU}(1)} 1_{(N_{f_{ter}} - i^{ter}_{PU}(1)) > 0)}$
$p^2_{t_{arr}}$	$\lambda^{ter}_{PU} \frac{i^{ter}_{SU}(1)}{N_{f_{ter}} - i^{ter}_{PU}(1)} 1_{((N_{f_{ter}} - i^{ter}_{PU}(1)) > 0) \wedge (idle^{ter}(1) > 0))}$
$p^3_{t_{arr}}$	$\lambda^{ter}_{PU} \frac{i^{ter}_{SU}(1)}{N_{f_{ter}} - i^{ter}_{PU}(1)} 1_{((N_{f_{ter}} - i^{ter}_{PU}(1)) > 0) \wedge (idle^{ter}(1) == 0))}$
$p^4_{t_{arr}}$	$\lambda^{ter}_{PU} \frac{i^{BS}_{HU}(1)}{N_{f_{ter}} - i^{ter}_{PU}(1)} 1_{((N_{f_{ter}} - i^{ter}_{PU}(1)) > 0) \wedge (idle^{ter}(1) > 0))}$
$p^5_{t_{arr}}$	$\lambda^{ter}_{PU} \frac{i^{BS}_{HU}(1)}{N_{f_{ter}} - i^{ter}_{PU}(1)} 1_{((N_{f_{ter}} - i^{ter}_{PU}(1)) > 0) \wedge (idle^{ter}(1) == 0))}$
$p^6_{t_{arr}}$	$\lambda^{ter}_{PU} \frac{i^{D}_{HU}(1)}{N_{f_{ter}} - i^{ter}_{PU}(1)} 1_{((N_{f_{ter}} - i^{ter}_{PU}(1)) > 0) \wedge (idle^{ter}(1) > 0))}$
$p^7_{t_{arr}}$	$\lambda^{ter}_{PU} \frac{i^{D}_{HU}(1)}{N_{f_{ter}} - i^{ter}_{PU}(1)} 1_{((N_{f_{ter}} - i^{ter}_{PU}(1)) > 0) \wedge (idle^{ter}(1) == 0))}$
$p^8_{t_{arr}}$	$\lambda^{ter}_{PU} \frac{idle^{ter}(6)}{N_{f_{ter}} - i^{ter}_{PU}(6)} 1_{((N_{f_{ter}} - i^{ter}_{PU}(6) > 0) \wedge (i^{ter}_{PU}(1) > 0))}$
$p^9_{t_{arr}}$	$\lambda^{ter}_{PU} \frac{i^{ter}_{SU}(6)}{N_{f_{ter}} - i^{ter}_{PU}(6)} 1_{((N_{f_{ter}} - i^{ter}_{PU}(6) > 0) \wedge (idle^{ter}(6) > 0) \wedge (i^{ter}_{PU}(1) > 0))}$
$p^{10}_{t_{arr}}$	$\lambda^{ter}_{PU} \frac{i^{ter}_{SU}(7)}{N_{f_{ter}} - i^{ter}_{PU}(7)} 1_{((N_{f_{ter}} - i^{ter}_{PU}(7) > 0) \wedge (idle^{ter}(7) == 0) \wedge (i^{ter}_{PU}(1) > 0) \wedge (i^{ter}_{SU}(1) < T))}$
$p^{11}_{t_{arr}}$	$\lambda^{ter}_{PU} \frac{i^{BS}_{HU}(6)}{N_{f_{ter}} - i^{ter}_{PU}(6)} 1_{((N_{f_{ter}} - i^{ter}_{PU}(6) > 0) \wedge (idle^{ter}(6) > 0) \wedge (i^{ter}_{PU}(1) > 0))}$
$p^{12}_{t_{arr}}$	$\lambda^{ter}_{PU} \frac{i^{BS}_{HU}(8)}{N_{f_{ter}} - i^{ter}_{PU}(8)} 1_{((N_{f_{ter}} - i^{ter}_{PU}(8) > 0) \wedge (idle^{ter}(8) == 0) \wedge (i^{ter}_{PU}(1) > 0) \wedge (i^{BS}_{HU}(1) < T))}$
$p^{13}_{t_{arr}}$	$\lambda^{ter}_{PU} \frac{i^{D}_{HU}(6)}{N_{f_{ter}} - i^{ter}_{PU}(6)} 1_{((N_{f_{ter}} - i^{ter}_{PU}(6) > 0) \wedge (idle^{ter}(6) > 0) \wedge (i^{ter}_{PU}(1) > 0))}$
$p^{14}_{t_{arr}}$	$\lambda^{ter}_{PU} \frac{i^{D}_{HU}(9)}{N_{f_{ter}} - i^{ter}_{PU}(9)} 1_{((N_{f_{ter}} - i^{ter}_{PU}(9) > 0) \wedge (idle^{ter}(9) == 0) \wedge (i^{ter}_{PU}(1) > 0) \wedge (i^{D}_{HU}(1) < T))}$
$p^1_{t_{dept}}$	$(i^{ter}_{PU}(1) + 1)\mu^{ter}_{PU} 1_{(idle^{ter}(1) > 0)}$
$p^2_{t_{dept}}$	$i^{ter}_{PU}(1)\mu^{ter}_{PU}$

$p^{6}_{t_{arr}}$ and $p^{13}_{t_{arr}}$ are the labels of the transitions where PU arrives at an HU occupied frequency retrieving content from another HU device and HU is moved to an idle channel. $p^{7}_{t_{arr}}$ and $p^{14}_{t_{arr}}$ are the labels of the transitions where PU arrives at an HU occupied frequency retrieving content from another HU device and HU is dropped due to the lack of idle frequency at the terrestrial link.

4.6.2. SU Transitions

Now we can continue our investigation of the system changes due to the SU service requests and completions. Assume that the State 1 in Figure 4.4 is a valid state.

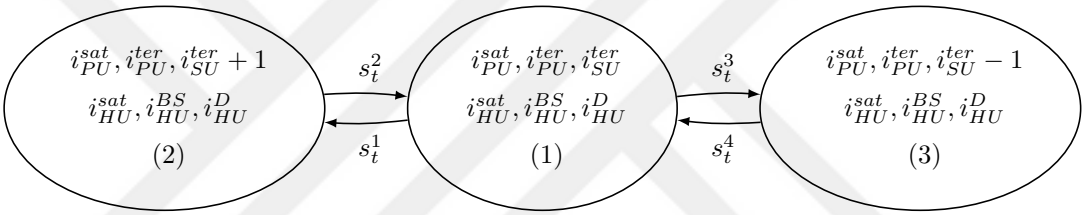


Figure 4.4: SU transitions.

SU transitions at the terrestrial link are labeled with s^x_t where $x \in \{1, 2, 3, 4\}$. The corresponding values are shown in the Table 4.5 with the corresponding type. At the terrestrial link SUs can arrive only when idle frequencies exist in the system which can be seen at s^1_t and s^4_t transition label values.

Table 4.5: SU transitions.

Variable	**Value**	**Type**
s^1_t	$\lambda^{ter}_{SU} 1_{(idle^{ter}(1)>0)}$	Arrival
s^2_t	$(i^{ter}_{SU}(1)+1)\mu^{ter}_{SU} 1_{(idle^{ter}(1)>0)}$	Departure
s^3_t	$i^{ter}_{SU}(1)\mu^{ter}_{SU}$	Departure
s^4_t	$\lambda^{ter}_{SU} 1_{((idle^{ter}(3)>0)\&(i^{ter}_{SU}(1)>0))}$	Arrival

4.6.3. HU Transitions

The investigation of the system changes due to the HU service requests and completions is given below. Assume that the State 1 in Figure 4.5 is a valid state.

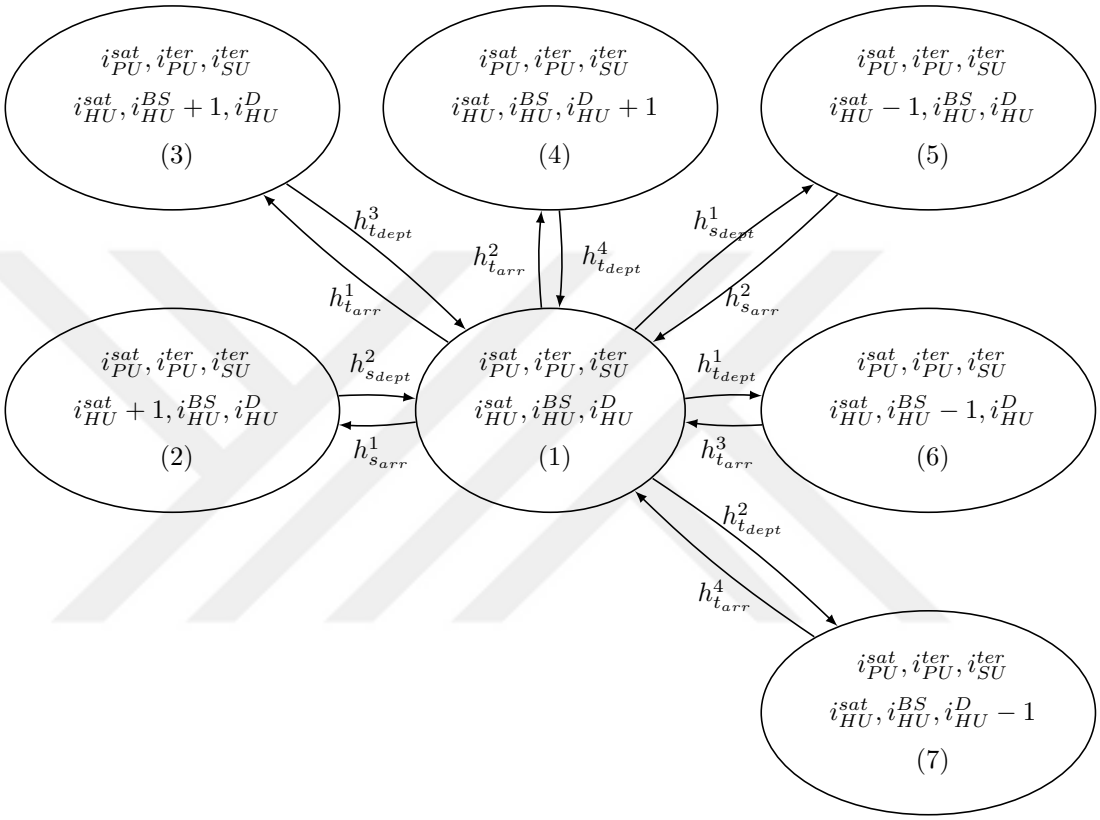


Figure 4.5: HU transitions.

To be able to understand HU arrival transitions, we need to understand preference coefficient and content availability parameters as shown in Table 4.6. The resource allocation is done according to a scheme in which each system component is assigned a preference coefficient to be chosen for content retrieval. In other words, the preference coefficients determine the likelihood of whether satellite, BS or device will be selected for content fetch operation. Additionally, this scheme has to take the content availabilities into account. Satellite, BS and HU devices have caches. The probability of finding a content at some of these system components is proportional to the cache size of the component.

Now let us define $R_{sat}(x)$, $R_{BS}(x)$, $R_{D2D}(x)$ and $R(x)$ for some state x as follows:

$$R_{sat}(x) := r_{sat} \cdot idle^{sat}(x) \tag{4.17}$$

$$R_{BS}(x) := r_{BS} \cdot idle^{ter}(x) \tag{4.18}$$

$$R_{D2D}(x) := r_{dev} \cdot idle^{ter}(x) \tag{4.19}$$

$$R(x) := R_{sat}(x) + R_{BS}(x) + R_{D2D}(x) \tag{4.20}$$

Let us give an example to describe how HU arrival transitions are computed. Assume that $r_{sat} = 1$, $r_{BS} = 2$, $r_{dev} = 10$, $idle^{sat}(x) = 2$, $idle^{ter}(x) = 3$ for some state x, $\mathbb{P}^v_{sat} = 0.5$, $\mathbb{P}^v_{BS} = 0.1$ and $\mathbb{P}^v_{dev} = 0.2$. Then each arrived HU content request is chosen to use satellite link with probability $\frac{R_{sat}(x)\mathbb{P}^v_{sat}}{R(x)} = \frac{1\times2\times0.5}{1\times2+2\times3+10\times3}$, use terrestrial link retrieving content from the BS with probability $\frac{R_{BS}(x)\mathbb{P}^v_{BS}}{R(x)} = \frac{2\times3\times0.1}{1\times2+2\times3+10\times3}$, use terrestrial link retrieving content from another HU device with probability $\frac{R_{D2D}(x)\mathbb{P}^v_{dev}}{R(x)}$ $= \frac{10\times3\times0.2}{1\times2+2\times3+10\times3}$. Note that with probability $\frac{R_{sat}(x)(1-\mathbb{P}^v_{sat})}{R(x)}$ the satellite link is chosen for the content retrieval but the content is not found at the satellite so the content retrieval does not occur and the system state does not change.

Table 4.6: Content availability and preference coefficient parameters.

Cache Size		Content Availability		Preference Coefficient	
$Cache_{sat}$	32 Gbits	$\mathbb{P}^v_{sat}$	0.427	r_{sat}	1
$Cache_{BS}$	8 Gbits	$\mathbb{P}^v_{BS}$	0.107	r_{BS}	2
$Cache_{Dev}$	200 Mbits	$\mathbb{P}^v_{dev}$	0.206	r_{dev}	10

HU arrival transitions at the satellite link are labeled with $h^x_{s_{arr}}$ where $x \in \{1, 2\}$ while arrival transitions at the terrestrial link are labeled with $h^x_{t_{arr}}$ where $x \in \{1, 2, 3, 4\}$. The corresponding values are shown in the Table 4.7. Labels $h^1_{s_{arr}}$ and $h^2_{s_{arr}}$ correspond to the transitions where HU arrives at a satellite link retrieving content from the satellite. $h^1_{t_{arr}}$ and $h^3_{t_{arr}}$ are the labels of the transitions where HU arrives at a terrestrial link retrieving content from the BS. $h^2_{t_{arr}}$ and $h^4_{t_{arr}}$ are the labels

of the transitions for D2D transmission where HU arrives at a terrestrial link retrieving content from another HU device.

Table 4.7: HU arrival transitions.

Variable	**Value**
$h^1_{s_{arr}}$	$\lambda_{HU}\frac{R_{sat}(1)\mathbb{P}^v_{sat}}{R(1)}1_{(R(1)>0)}$
$h^2_{s_{arr}}$	$\lambda_{HU}\frac{R_{sat}(5)\mathbb{P}^v_{sat}}{R(5)}1_{((i^{sat}_{HU}(1)>0)\wedge(R(5)>0))}$
$h^1_{t_{arr}}$	$\lambda_{HU}\frac{R_{BS}(1)\mathbb{P}^v_{BS}}{R(1)}1_{(R(1)>0)}$
$h^2_{t_{arr}}$	$\lambda_{HU}\frac{R_{D2D}(1)\mathbb{P}^v_{dev}}{R(1)}1_{(R(1)>0)}$
$h^3_{t_{arr}}$	$\lambda_{HU}\frac{R_{BS}(6)\mathbb{P}^v_{BS}}{R(6)}1_{((i^{BS}_{HU}(1)>0)\wedge(R(6)>0))}$
$h^4_{t_{arr}}$	$\lambda_{HU}\frac{R_{D2D}(7)\mathbb{P}^v_{dev}}{R(7)}1_{((i^{D}_{HU}(1)>0)\wedge(R(7)>0))}$

HU departure transitions at the satellite link are labeled with $h^x_{s_{dept}}$ where $x \in \{1,2\}$ while departure transitions at the terrestrial link are labeled with $h^x_{t_{dept}}$ where $x \in \{1,2,3,4\}$. The corresponding values are shown in the Table 4.8. Labels $h^1_{s_{dept}}$ and $h^2_{s_{dept}}$ correspond to the transitions where HU that retrieves content from the satellite departs from some satellite link and that link becomes idle. $h^1_{t_{dept}}$ and $h^3_{t_{dept}}$ are the labels of the transitions where HU that retrieves content from the BS departs from some terrestrial link and that link becomes idle. $h^2_{t_{dept}}$ and $h^4_{t_{dept}}$ are the labels of the transitions where HU that retrieves content from another HU device departs from some terrestrial link and that link becomes idle.

Table 4.8: HU departure transitions.

Variable	**Value**
$h^1_{s_{dept}}$	$i^{sat}_{HU}(1)\mu^{s}_{HU}$
$h^2_{s_{dept}}$	$i^{sat}_{HU}(2)\mu^{sat}_{HU}1_{(idle^{sat}(1)>0)}$
$h^1_{t_{dept}}$	$i^{BS}_{HU}(1)\mu^{BS}_{HU}$
$h^2_{t_{dept}}$	$i^{D}_{HU}(1)\mu^{D}_{HU}$
$h^3_{t_{dept}}$	$i^{BS}_{HU}(3)\mu^{BS}_{HU}1_{(idle^{ter}(1)>0)}$
$h^4_{t_{dept}}$	$i^{D}_{HU}(4)\mu^{D}_{HU}1_{(idle^{ter}(1)>0)}$

4.7. Balance Equations

To be able to find the steady state probabilities of each state, we have to write down the balance equations of our system for each valid state. For simplicity the state (x) at figure y will be denoted as S^y_x. Now, let us start constructing a balance equation as follows:

$$LHS_{PU} := \pi_{(S^{4.2}_1)}(p^1_s + p^3_s + \sum_{i=1}^{7} p^i_{t_{arr}} + p^2_{t_{dept}}) \tag{4.21}$$

$$LHS_{SU} := \pi_{(S^{4.2}_1)}(s^1_t + s^3_t) \tag{4.22}$$

$$LHS_{HU} := \pi_{(S^{4.2}_1)}(h^1_{s_{arr}} + \sum_{i=1}^{2} h^i_{t_{arr}} + h^1_{s_{dept}} + \sum_{i=1}^{2} h^i_{t_{dept}}) \tag{4.23}$$

$$RHS^s_{PU} := \pi_{(S^{4.2}_2)}(p^2_s) + \pi_{(S^{4.2}_3)}(p^4_s) \tag{4.24}$$

$$RHS^t_{PU} := \sum_{i=0}^{2}(\pi_{(S^{4.3}_6)}p^{9+2i}_{t_{arr}}) + \sum_{i=0}^{2}(\pi_{(S^{4.3}_{i+7})}p^{2(i+5)}_{t_{arr}}) + \pi_{(S^{4.3}_2)}(p^1_{t_{dept}}) \tag{4.25}$$

$$RHS_{SU} := \pi_{(S^{4.4}_2)}(s^2_t) + \pi_{(S^{4.4}_3)}(s^4_t) \tag{4.26}$$

$$RHS_{HU} := \sum_{i=0}^{1}(\pi_{(S^{4.5}_{i+6})}h^{i+3}_{t_{arr}}) + \pi_{(S^{4.5}_5)}h^2_{s_{arr}} + \pi_{(S^{4.5}_2)}h^2_{s_{dept}} + \sum_{i=0}^{1}(\pi_{(S^{4.5}_{i+3})}h^{i+3}_{t_{dept}}) \tag{4.27}$$

$$LHS_{PU} + LHS_{SU} + LHS_{HU} = RHS^s_{PU} + RHS^t_{PU} + RHS_{SU} + RHS_{HU} \tag{4.28}$$

For each state we derive the balance equation and solve the resulting set of balance equations. Finally, we find the steady state probabilities of being at each state.

4.8. Performance Metrics

4.8.1. Throughput

The throughput of some user type at some link is defined to be the rate at which the number of content requests of that user type at the corresponding link are completed. Now, let us give the definitions of throughput as follows.

$$Th_{PU}^{y} := \sum_{x \in S} i_{PU}^{y}(x)\mu_{PU}^{y}\pi_x \text{ where } y \in \{sat, ter\} \tag{4.29}$$

$$Th_{SU}^{ter} := \sum_{x \in S} i_{SU}^{ter}(x)\mu_{SU}^{ter}\pi_x \tag{4.30}$$

$$Th_{HU}^{y} := \sum_{x \in S} i_{HU}^{y}(x)\mu_{HU}^{y}\pi_x \text{ where } y \in \{sat, BS, D\} \tag{4.31}$$

Then the total throughput of HUs is

$$Th_{HU} := Th_{HU}^{sat} + Th_{HU}^{BS} + Th_{HU}^{D} \tag{4.32}$$

4.8.2. Energy Efficiency

The energy consumption per each successfully sent bit (EPB) in the system for HUs is used to show the energy efficiency in Joule per bit (Jpb). For each state the total power consumed by system components is calculated in the nominator of Equation 4.33. The average service rate for the mean base content for each state is calculated in the denominator of Equation 4.33.

$$EPB_{HU} := \sum_{x \in S} \frac{(i_{HU}^{sat}(x)P_{sat}^{ch} + i_{HU}^{BS}(x)P_{BS}^{ch} + i_{HU}^{D}(x)P_{dev}^{tx})}{s(\hat{HU}, v_b)(i_{HU}^{sat}(x)\mu_{HU}^{sat} + i_{HU}^{BS}(x)\mu_{HU}^{BS} + i_{HU}^{D}(x)\mu_{HU}^{D})}\pi_x \tag{4.33}$$

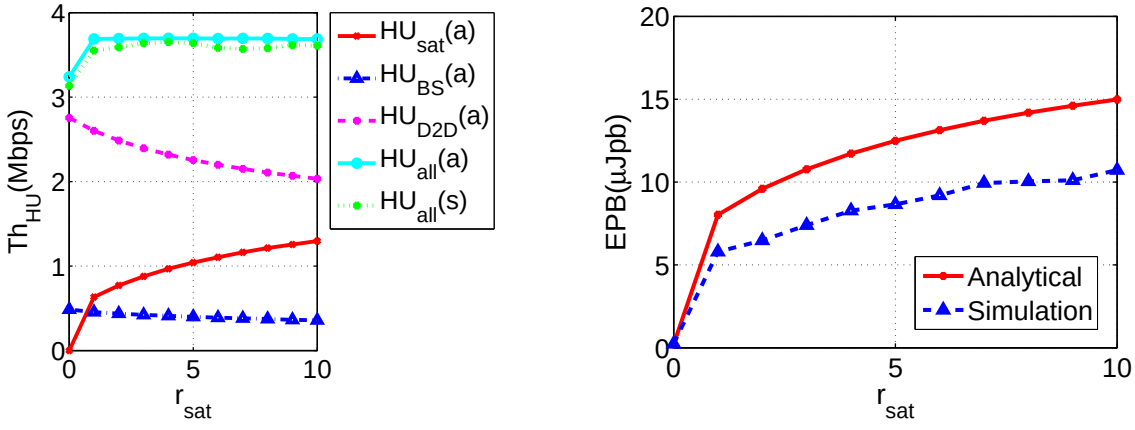
4.9. Performance Evaluation without Caching in the System

Initially we have investigated our system as if there is no cache mechanism in system components: the satellite, the BS and HU devices. We analyze the effects of two main system parameters, namely mode selection and PU traffic activity, on system performance represented with throughput and energy efficiency.

We adopt one additional approach for evaluating our analytical model. In addition to our analytical results (baseline analysis), we also simulate the analytical model to generate simulation results which are basically experimental results for simulated analytical model. We set the preference coefficients as in Table 4.6 as the default setting.

4.9.1. Effect of Mode Preference: Satellite, BS or D2D

For the HU resource allocation analysis, different preference coefficients for different content holders are investigated. From Figure 4.6(a) we see that with larger satellite preference coefficient, the throughput of HUs retrieving content from the satellite increase while the throughput of HUs retrieving content from the BS or another HU device decreases. The probability that a content can be found at some device is higher than the probability that it can be found at the BS. Additionally, the preference coefficient of D2D is higher. Since the contribution of the D2D is higher than the BS, the preference shifting towards the satellite leads to bigger decrease in D2D mechanism as can be seen by Figure 4.6(a). The total analytical throughput is verified by the corresponding simulation. As the satellite link has the lowest channel capacity, the increased satellite preference leads to more energy consumption for the same amount of information transmission. This result can be seen at Figure 4.6(b). The results for the analysis and its simulation follow the same trend. However, the baseline analytical results have higher values. Thus they serve as upper bound for our system.

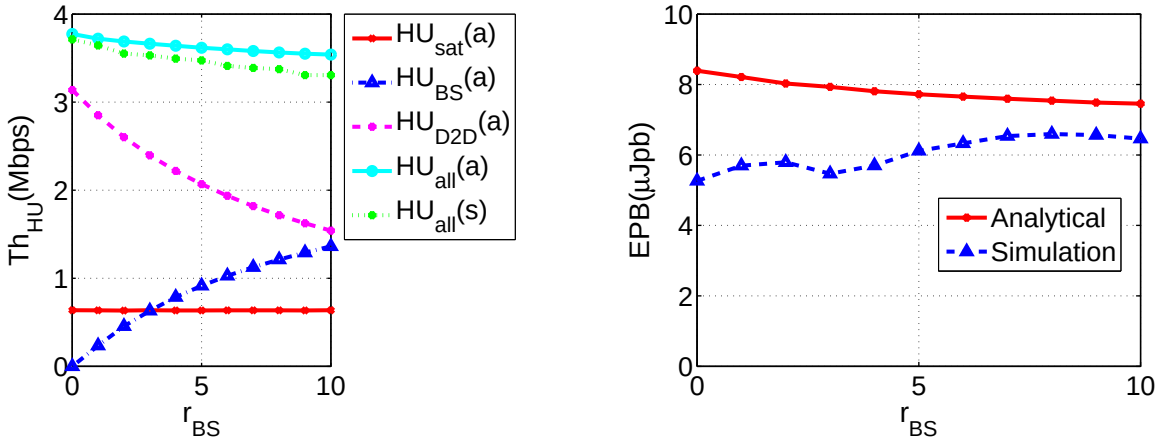


(a) Throughput of HUs (a: analytical, s: simulation).

(b) EPB.

Figure 4.6: Effect of increasing satellite preference parameter.

From Figure 4.7(a) we see that with increasing BS preference coefficient, the throughput of HUs retrieving content from the BS is increased while the throughput of HUs through the D2D mechanism is reduced. The reason is since the content retrieval mode at the terrestrial link is provided by either BS or some HU device as the default preference coefficient for the D2D is 10 and BS preference coefficient increases up to 10, their contributions at the throughput become closer. The satellite link is not affected. We were expecting to see that both the satellite and D2D activity is suppressed. However, it has a higher content availability probability compared to other system components therefore it is favorable. Besides, satellite is already given a low preference coefficient value and there are less number of frequencies in the satellite channel, so it is less preferred by new requests. Therefore its usage is not affected as the D2D mechanism. The overall throughput of the analytical analysis for the system has the same trend with and similar values for the corresponding simulation as shown in Figure 4.7(a). Energy efficiency results of the analysis and simulation converge to each other with increased BS preference coefficient as shown in Figure 4.7(b).

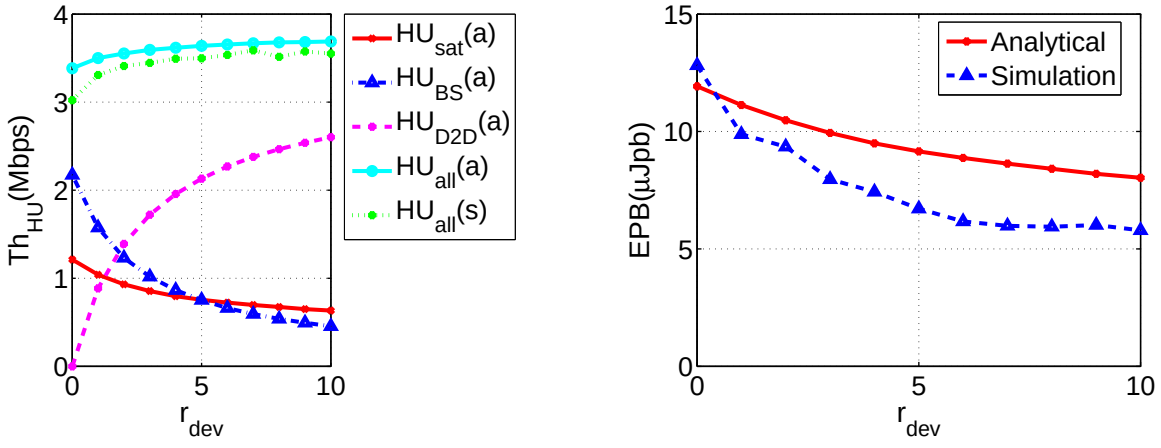


(a) Throughput of HUs (a: analytical, s: simulation).

(b) EPB.

Figure 4.7: Effect of increasing BS preference parameter.

With increasing D2D preference, the throughput of HUs retrieving content from another HU device increases while the throughput of HUs retrieving content from the satellite or BS decreases as seen in Figure 4.8(a). Note that the decrease in the BS is higher than the decrease in the satellite. The reason is that the content availability of the satellite is four times higher than the other one even though its preference coefficient is half of the BS. Additionally, the D2D mechanism and the BS share the terrestrial link. However, the overall throughput increases. As the D2D mechanism has small service duration, the terrestrial frequencies can be idle for longer time and new requests can be served successfully. Additionally, the analytical and simulation results are consistent with each other. The energy consumption per successfully sent bit is reduced as seen in Figure 4.8(b). The reason is that the D2D mechanism consumes less energy for the same amount of information transmission compared to other mechanisms. The analytical and corresponding simulation results again follow the same trend for the energy consumption per successfully sent bit over the system.



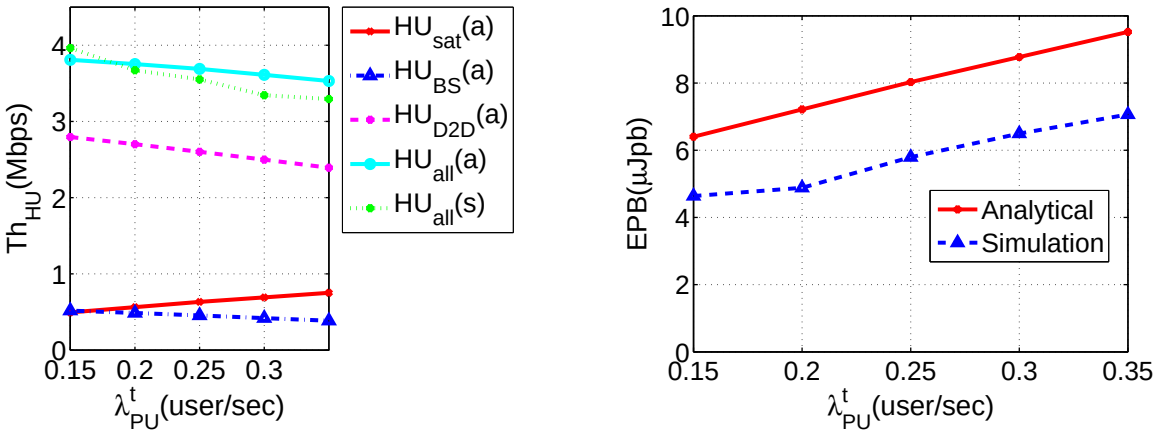
(a) Throughput of HUs (a: analytical, s: simulation).

(b) EPB.

Figure 4.8: Effect of increasing D2D preference parameter.

4.9.2. Effect of PU Traffic Activity (Changing $\lambda_{\mathrm{PU}}^{\mathrm{ter}}$)

Increasing $\lambda_{\mathrm{PU}}^{\mathrm{ter}}$ leads to higher preference of the satellite link as there will be more PUs at the terrestrial link. This is seen in Figure 4.9(a). Note that the terrestrial link will be much more occupied by the PUs and can serve less HUs. More of the HU requests will be tried to be served by the satellite link but the service capacity of the satellite link is low. Hence, the overall throughput of the system decreases. The resource allocation preference shift towards the satellite leads to decreased energy efficiency of HUs as shown in Figure 4.9(b). This is caused by the satellite link having the lowest channel capacity in the system. For the same amount of information, more power is consumed at the satellite link due to channel characteristics. Note that the baseline analytical and corresponding simulation results follow the same pattern. Analytical results have greater values than the corresponding simulation as in the previous experiments.



(a) Throughput of HUs (a: analytical, s: simulation).

(b) EPB.

Figure 4.9: Effect of increasing PU arrival rate at terrestrial link.

4.10. Analytical Results with Integrated Caching Mechanism

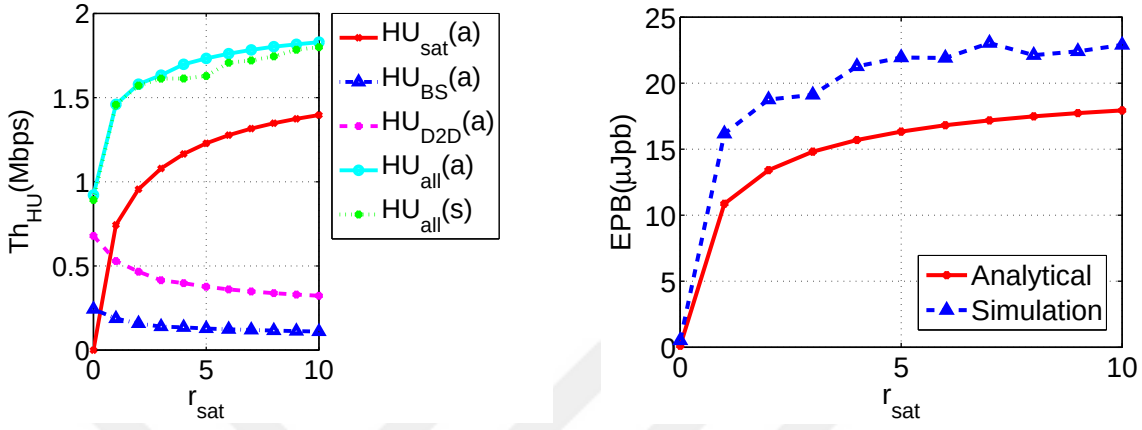
Caching is essential for content-centric operation [37]. In this section, we investigate the effect of caching on our system. We integrate a streamlined caching mechanism into our network to see how the system will behave in a much more realistic situation in our analysis. We set the preference coefficients all equal to one as the default setting.

4.10.1. Effect of Mode Preference: Satellite, BS or D2D

For the HU resource allocation analysis, different preference coefficients for different content holders are to be investigated. These configurations are evaluated in terms of throughput and energy efficiency metrics.

From Figure 4.10(a) we see that with increasing satellite preference coefficient, the throughput of HUs retrieving content from the satellite is increased while the throughput of HUs retrieving content from the BS or another HU device is decreased. The decrease at D2D mechanism is steeper compared to the decrease at the BS usage. As the satellite link has the lowest channel capacity, the increased satellite preference leads to more energy consumption for the same amount of successful information transmis-

sion. This phenomenon can be seen at Figure 4.10(b). Both instances follow the same trend pattern.

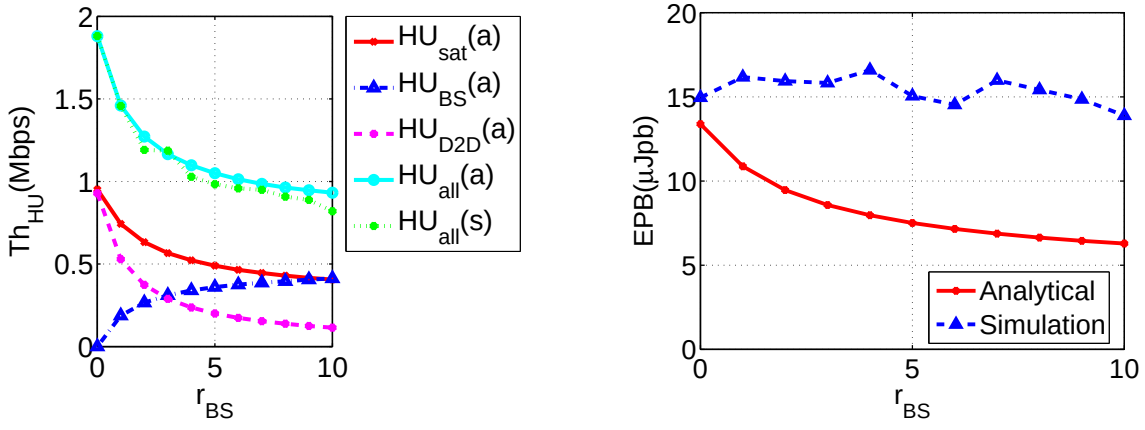


(a) Throughput of HUs (a: analytical, s: simulation).

(b) EPB.

Figure 4.10: Effect of increasing satellite preference parameter.

From Figure 4.11(a) we see that with increasing BS preference coefficient, the throughput of HUs retrieving content from the BS is increased while the throughput of HUs retrieving content from the satellite or using D2D mechanism is decreased as expected. However, the overall throughput is decreased. At the satellite link although the channel characteristics do not allow high content transmission rate, its preference decrease leads to smaller throughput since the cache size of the satellite is the largest among all system components. Additionally, the D2D mechanism is less preferred due to increased BS preference coefficient. This situation also has a negative affect on the overall throughput. Since the content availability of the BS is the lowest among all system components, the overall throughput is again decreased. On the energy efficiency dimension, the perfomance is improved due to decrease in the satellite usage. Note that the decrease in the analytical analysis is steeper than the corresponding simulation.

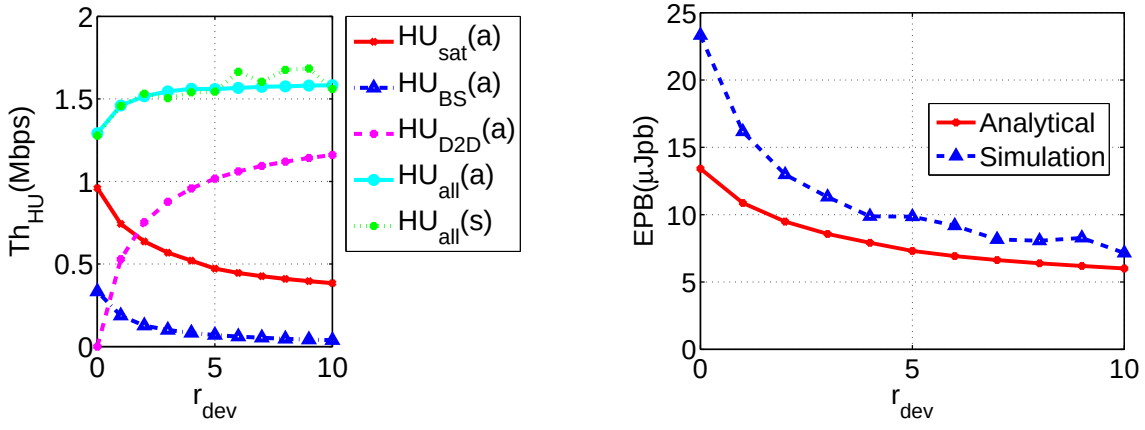


(a) Throughput of HUs (a: analytical, s: simulation).

(b) EPB.

Figure 4.11: Effect of increasing BS preference parameter.

Increasing D2D preference coefficient increases the throughput of HUs retrieving content from another HU device while the throughput of HUs retrieving content from the satellite or BS is decreased as seen in Figure 4.12(a). The overall throughput increases since offloading content retrieval towards the D2D mechanism makes the channel have many more idle frequencies which can be used by newly arrived HU content requests leading to higher throughput for HUs. The energy consumption per successfully sent bit is reduced as seen in Figure 4.12(b). The D2D mechanism consumes less energy for the same amount of information transmission compared to other mechanisms. Therefore, we observe less energy consumption for the same amount of successfully transmitted bits. This is in line with expectations since D2D transmission utilizes spatial locality for more efficient communications.



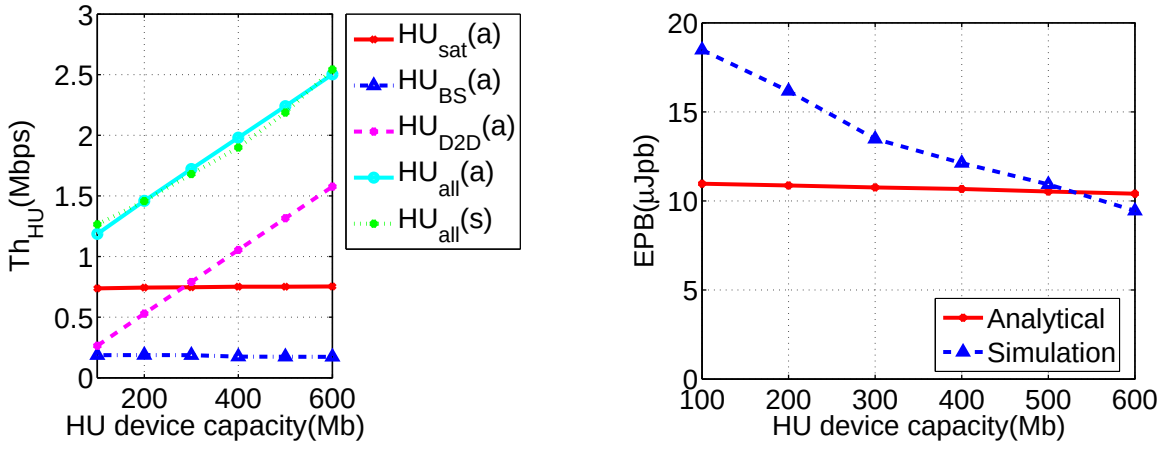
(a) Throughput of HUs (a: analytical, s: simulation).

(b) EPB.

Figure 4.12: Effect of increasing D2D preference parameter.

4.10.2. Effect of Cache Size ($\mathbf{Cache_{HU}}$)

The concept of caching and in-network storage are paramount for content-centric operation. Therefore, the caching characteristics and operation are important research questions. In this analysis, we focus on the most fundamental attribute of such a capability which is cache size. With increasing cache capacities of HU devices, the probability of finding content at an HU device is increased. Moreover, the throughput of HUs retrieving content from another HU device and overall throughput of HUs both improve as shown in Figure 4.13(a). Increased HU device capacity reduces the energy consumption per successfully sent bit due to throughput increase by D2D usage as shown in 4.13(b). Although the decrease is marginal for analytical results, it is more evident in the simulation.



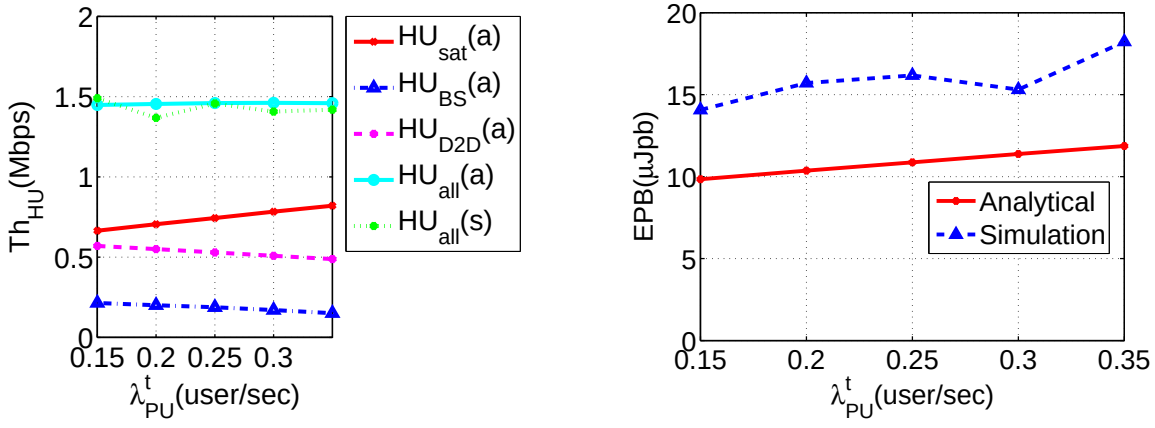
(a) Throughput of HUs (a: analytical, s: simulation).

(b) EPB.

Figure 4.13: Effect of increasing HU device cache size.

4.10.3. Effect of PU Traffic Activity (Changing $\lambda_{\mathrm{PU}}^{\mathrm{ter}}$)

Increasing $\lambda_{\mathrm{PU}}^{\mathrm{ter}}$ leads to preference shifting to the satellite link as there will be more PUs at the terrestrial link. The contribution of other mechanisms decreases but the overall throughput is not affected. This is evident in Figure 4.14(a). The resource allocation preference shift towards the satellite leads to decreased energy efficiency of HUs as shown in Figure 4.14(b). The reason is that the satellite link has the lowest channel capacity in the system. For the same amount of information, more power is consumed at the satellite link due to channel characteristics.



(a) Throughput of HUs (a: analytical, s: simulation).

(b) EPB.

Figure 4.14: Effect of increasing PU arrival rate at terrestrial link.

The experimental results indicate the advantages of D2D communications for exploiting locality and CR paradigm for spectral capacity. Moreover, the satellite segment provides one more degree of freedom for maintaining communications despite the fact that it may deteriorate energy efficiency in some situations.

5. SIMULATION BASED INVESTIGATION

The simulation based investigation considers the system in analytical evaluation but with more practical aspects such as traffic model, layered content, and content quality. To reiterate, we assume that there are two main segments in the network, namely satellite and terrestrial. We assume that there is one satellite at frequency level f_{sat} with bandwidth W_{sat}. The terrestrial system is at frequency level f_{ter} with bandwidth W_{ter}. There is one BS and we investigate the area of that BS cell although the simulation can be extended to larger topologies.

In this model, there are three types of users, namely PUs, SUs and HUs as explained in Section 4.1. The resource allocation is done centrally by the BS. It allocates resources to HUs taking frequency state into account. That is, the central entity can detect the PU, SU and HU arrivals and departures and it can allocate resources to HUs accordingly. Moreover, the central controller has knowledge on the active HUs. No spectral overlay is allowed (a frequency cannot be used by two different users at the same time). For the resource allocation to new HU content requests, currently active HUs are not allowed to be used by the controller since each HU has a single RF front-end.

5.1. Content Model

A content is assumed to be a self-contained chunk of video. Each content requested by an HU in our system has the following features.

(i) Identifier: a unique id for content
(ii) Content holder(s): the entities where the content is available
(iii) Size: the size of the content for doing necessary operations such as cache replacement
(iv) Popularity rank: used for popularity related simulations
(v) Priority: value which is identical for all base and enhancement contents (the

popularity of base contents are higher than enhancement counterparts)

The contents can be cached at the satellite, the BS and/or HU device(s). As in Section 4.2, an entire content is assumed to be at the same place. i.e. It is not allowed that some portion is in the satellite while the rest is in an HU device. There is also the "universal source" concept which is a s a logical shorthand representation for chunk stores/servers outside of our network but in the rest of Internet. It corresponds to the case where the content can not be found in the local nodes. The cache mechanism works as an in-network storage mechanism in network anchoring points. If requested content is not found anywhere and retrieved from the universal source via the satellite link, it is cached at the satellite. If requested content is not found anywhere and retrieved from the universal source via terrestrial link through the BS, it is cached at the BS as long as all the content is retrieved via the BS.

At the end user side, if the requested content is successfully retrieved by some HU, it is cached at that HU device. For the cache operation, Least Recently Used (LRU) replacement algorithm is used. If there is enough storage in the cache for the arrived content, it is readily inserted into the cache. Otherwise the least recently used content is discarded. The algorithm continues evicting least recently used contents until there is enough space in the cache for the recently arrived content.

For the simulation based investigation, we integrate layered content concept into the system for our analysis at the application layer. Each content is either of type *base* or *enhancement*. The base contents are composed of the standard components of a content whereas enhancement contents have extra components for high quality service. Being of type base or enhancement defines the priority of a content. Base contents have higher priority over enhancement contents. How this characteristic affects the resource allocation is studied in the Section 5.4.

The content identifier is required to uniquely define each content in the system. Base contents have odd identifiers whereas enhancement contents have even identifiers. When base content has identifier x, then x+1 is the identifier of the corresponding

enhancement content.

Content sizes are determined according to exponential distribution with mean content size specified as a parameter. PU and SU content requests are only of type base whereas HU content requests can be of type base or enhancement. Mean base content size parameter in our system is higher compared to mean enhancement content size parameter.

Some contents are frequently requested while some others are rarely requested. This phenomenon can be modeled via popularity ranking. For this purpose, Zipf distribution is used. The cumulative distribution function (CDF) of zipf distribution is $CDF(k,s) = \frac{H_{k,s}}{H_{V,s}}$ where k is the popularity rank of the base content, s is the exponent characterizing the distribution and V is the total number of base contents. During each HU content request generation a random number from $[0,1]$ interval is chosen, say y. The value of k such that randomly chosen number y falls between $CDF(k-1,s)$ and $CDF(k,s)$ gives the popularity rank of HU base content request among all base contents. Hence, the base content with popularity rank k is requested. Enhancement content request generation is handled in a different way. HU users are said to be either low or high quality (HQ) consumer. The ratio of HQ HUs is a system parameter. After each successfully retrieved base content, receiver generates enhancement content request if the receiver is a HQ HU. Otherwise no enhancement content request is generated. Some number of most popular contents are cached at the satellite and the BS as long as the cache capacity is not exceeded.

5.2. Traffic Model

Initially we generate PU traffic streams at the satellite link and at the terrestrial link as Poisson arrival process with mean arrival rate $\lambda_{PU_{sat}}$ and $\lambda_{PU_{ter}}$ respectively. As SUs are assumed to be active at terrestrial link, we generate SU traffic at terrestrial link as Poisson arrival process with mean arrival rate $\lambda_{SU_{ter}}$.

When an HU out of N_{HU} HUs arrives to the system, it requests some content

according to a popularity model of contents as shown in Section 5.1. The arrival process of HUs are again Poisson with mean arrival rate λ_{HU}.

Due to the PU appearance, HU content retrievals can be interrupted. HU can continue content retrieval from another content holder. For instance, HU starts content retrieval from the BS at some terrestrial frequency. However, once a PU appears at that frequency, HU preempts the frequency and continues content retrieval from the satellite.

5.3. Assumptions and Parameters

In the simulations as in the case of the analytical work, we consider non-time slotted scheme. We ignore the transmission errors, sensing errors and waiting times for the sake of simplicity. We consider the coverage of a BS, again as in the analytical model in Chapter 4. We assume that all the regions have the same arrival and service rates for all user types. Therefore, concentrating on one of the regions does not result in the loss of generality. We ignore content transmission retrials in case of unsuccessful transmissions as in the case of analytical analysis.

Table 5.1: Simulation parameters.

Parameter	**Value**	Explanation
T	1200 sec	Total simulation time
λ_{PU}^{sat}	0.15 $\frac{user}{sec}$	Arrival rate of PUs at satellite link
λ_{PU}^{ter}	0.8 $\frac{user}{sec}$	Arrival rate of PUs at terrestrial link
λ_{SU}^{ter}	0.5 $\frac{user}{sec}$	Arrival rate of SUs at terrestrial link
λ_{HU}	0.3 $\frac{user}{sec}$	Arrival rate of HUs at the system
W_{sat}	36 MHz	Bandwidth of satellite link
W_{ter}	2 MHz	Bandwidth of terrestrial link
f_{sat}	20 GHz	Frequency of satellite link
f_{ter}	700 MHz	Frequency of terrestrial link
$s(\hat{HU}, v_b)$	25 Mbits	Mean base content size requested by an HU
$s(\hat{HU}, v_e)$	5 Mbits	Mean enhancement content size requested by an HU
$s(\hat{PU^s}, v_b)$	25 Mbits	Mean base content size requested by a PU at satellite link
$s(\hat{PU^t}, v_b)$	25 Mbits	Mean base content size requested by a PU at terrestrial link
$s(\hat{SU}, v_b)$	25 Mbits	Mean base content size requested by a SU at terrestrial link
$Cache_{sat}$	32 Gbits	Satellite cache size
$Cache_{BS}$	8 Gbits	Base station cache size
$Cache_{Dev}$	200 Mbits	Hybrid device cache size
M	600 m	The diameter of the BS cell
N_0^{sat}	$10^{-18}\frac{Watt}{Hz}$	Noise at satellite link
N_0^{ter}	$1.5 \cdot 10^{-19}\frac{Watt}{Hz}$	Noise at terrestrial link
d_{BS}	$\frac{M}{4}$ m	Mean distance to the base station of a primary user, secondary user
d_{sat}(LEO)	300 km	Distance from satellite to earth

Table 5.2: Simulation parameters without unit.

Parameter	**Value**	Explanation
V	1000	Total number of contents
$N_{f_{sat}}$	5	Total number of satellite frequencies
$N_{f_{ter}}$	10	Total number of terrestrial frequencies
r_{sat}	1	Resource allocation preference coefficient for content retrieval from the satellite
r_{BS}	2	Resource allocation preference coefficient for content retrieval from the BS
r_{dev}	10	Resource allocation preference coefficient for content retrieval from an HU device
s_{zipf}	1	Zipf distribution parameter
b	5	$\frac{(b+1)}{2}$ base contents will be located at the satellite and BS unless size exceeds corresponding cache size
r_{enh}	0.5	The rate of HUs that request both base and enhancement contents
$r_{colocated}$	1	The rate at which base and corresponding enhancement contents are colocated at the same cache
u	1	Universal source existence indicator
c_{HU}	920	HU increase factor
G_{sat}	$2.5 \cdot 10^4$	Gain of the satellite
G_{BS}	$4 \cdot 10^{-5}$	Gain of the base station
$G_{dev(HU)}$	$6 \cdot 10^{-2}$	Gain of a hybrid user
$G_{dev(PU_{ter})}$	$11 \cdot 10^{-2}$	Gain of a primary user requesting service at terrestrial link

By the use of Friis and Shannon's formulae, we get the received power strength of

users that retrieve content from content holders and the channel capacities respectively. The parameters for the simulation are listed in Table 5.1 and Table 5.2. For the PUs and SUs, we do not focus on their specific physical locations and generate traffic according to the traffic model. To calculate transmission rate, we take the half of the radius as the distance to the BS for PUs retrieving content from the BS and SUs. In case of PUs retrieving content from the satellite, the transmission distance is d_{sat}. The traffic variability of PUs and SUs are achieved by exponentially distributed content sizes.

Note that $N_{HU} = N_{f_{sat}} + 2N_{f_{ter}} + c_{HU}$. The number of HUs in the system is bounded with a lower bound by $N_{f_{sat}}$ and $N_{f_{ter}}$ for arrivals being Poisson process. However, the system does not have Markovian property due to service interruptions and continuations in different links and/or frequencies. This requirement is relaxed in the simulation framework since we are not bound by tractability as in analytical approach.

5.4. Resource Allocation

The resource allocation is done such that an arrival or departure event triggers system change. At each change, current link state is updated accordingly.

5.4.1. PU Arrival at the Satellite Link

If there is at least an idle frequency at the satellite link, PU is allocated to one such idle satellite frequency randomly. The satellite link state is updated. If no idle frequency exists, PU is blocked. Then, the satellite link state is not changed.

5.4.2. PU Arrival at the Terrestrial Link

If no idle frequency exists at the terrestrial link, PU is blocked. If at least one frequency exists that has no PU activity, PU is allocated to one of those frequencies randomly. The terrestrial link state is updated. That frequency can be idle, have SU or HU in SU mode activity. If that frequency is idle then no preemption occurs.

Otherwise, SU or HU in SU mode retrieving content from the BS or another HU device is preempted. For the preempted user, a new event is created with the arrival time equal to the PU arrival time at the terrestrial link. Through the new event, the preempted user will try to get the rest of the content. The rest of the content is not necessarily taken through the same link and from the same content holder. For each new generated event, the process starts from the scratch.

5.4.3. SU Arrival at the Terrestrial Link

If at least one idle frequency is found at the terrestrial link, SU is allocated to one of the idle terrestrial frequencies randomly. The terrestrial link state is updated. If no idle frequency exists and the event corresponds to a new SU arrival, then SU is blocked. If no idle frequency exists and the event belongs to a preempted SU, then SU is dropped. The terrestrial link state is not changed in either case.

5.4.4. HU Arrival

If an HU finds the content in its own cache, it does not search it somewhere else. The terrestrial link state is not changed. For the LRU algorithm to work properly, the contents in the local cache of the HU device is reordered.

If the content is not found at the receiver HU device itself, the central controller, namely the BS, runs the following procedure: Look at the current content holders. If the content is found at some content holder, the corresponding idle frequencies are taken to be candidate for content retrieval. The likelihood of choosing some candidate is determined by its preference coefficient as in the case of analytical work. For the satellite, different preference coefficients of the BS and HU device(s) are to be investigated. For instance, how is the system affected if the D2D preference coefficient is taken to be high? If the content is found at the satellite, the idle frequencies at the satellite link are taken to be candidate for content retrieval from the satellite. Note that not all of the idle frequencies at the satellite link are taken to be candidates. As the satellite link is accessed by either PU or HU in PU mode in case of high HU activ-

ity, PUs will be blocked. To solve this problem, some idle frequencies at the satellite link are released from being candidate. If the content is found at the BS, the idle frequencies at the terrestrial link are taken to be candidate for content retrieval from the BS. If the content is found at an HU device, the idle frequencies at the terrestrial link are taken to be candidate for content retrieval through D2D mechanism.

Let us give an example. Say $N_{f_{sat}}$ is 5 and $N_{f_{ter}}$ is 10. There are three idle frequencies at the satellite link, say the third, fourth and fifth frequencies, four idle frequencies at the terrestrial link, say first, second, seventh and ninth frequencies. The busy frequencies are marked with zero and idle channels are marked with one as shown in Figures 5.1 and 5.2. Now assume that $r_{sat} = 1$, $r_{BS} = 2$ and $r_{dev} = 3$. The probability of getting content from the satellite is given as follows:

$$\frac{r_{sat} \cdot idle^{sat}(x)}{r_{sat} \cdot idle^{sat}(x) + r_{BS} \cdot idle^{ter}(x) + r_{dev} \cdot idle^{ter}(x)} = \frac{1 \cdot 3}{1 \cdot 3 + 2 \cdot 4 + 3 \cdot 4} \tag{5.1}$$

where x is the current state. The probability of getting content from the BS is

$$\frac{r_{BS} \cdot idle^{ter}(x)}{r_{sat} \cdot idle^{sat}(x) + r_{BS} \cdot idle^{ter}(x) + r_{dev} \cdot idle^{ter}(x)} = \frac{2 \cdot 4}{1 \cdot 3 + 2 \cdot 4 + 3 \cdot 4} \tag{5.2}$$

The probability of getting content from the satellite is

$$\frac{r_{dev} \cdot idle^{ter}(x)}{r_{sat} \cdot idle^{sat}(x) + r_{BS} \cdot idle^{ter}(x) + r_{dev} \cdot idle^{ter}(x)} = \frac{3 \cdot 4}{1 \cdot 3 + 2 \cdot 4 + 3 \cdot 4} \tag{5.3}$$

0	0	1	1	1

Figure 5.1: Satellite link state x.

1	1	0	0	0	0	1	0	1	0

Figure 5.2: Terrestrial link state x.

No candidate for content retrieval can happen due to two reasons. First, the

requested content can not be found at a content holder. Second, no idle frequency is available at some link. For instance, content is available at the satellite but the satellite link is fully busy. There are idle frequencies at the terrestrial link but content can not be found at the BS or any HU device. In this case, no candidate frequency for the content retrieval exists.

When no candidate is found, the operation is as follows. If content retrieval from the universal source is allowed, the central controller will try to retrieve the content to the satellite or the BS cache from the universal source. The idle frequencies at the satellite link are taken to be candidate for content retrieval from the satellite. Note that some idle frequencies at the satellite link are released from being candidate. The idle frequencies at the terrestrial link are taken to be candidate for content retrieval from the BS. The chance of choosing some candidate is determined by its preference coefficient as explained before. If the base content retrieval fails due to all candidate frequencies being busy, it will apply the replacement procedure. The replacement can be applied only to terrestrial frequencies that are used for enhancement content retrievals from the BS or another HU device. If there exists terrestrial frequencies that are used for enhancement content retrievals from the BS or another HU device, then the replacement will occur. If there do not exist terrestrial frequencies that are used for enhancement content retrievals from the BS or another HU device, then HU base content request is either blocked if content request is new or dropped if content transmission was preempted before. If enhancement content retrieval fails due to all candidate frequencies being busy, it will be either blocked if content request is new or dropped if content transmission was preempted before.

If the content retrieval from the universal source is not allowed and content is of type base, it will use the replacement procedure. If the content retrieval from the universal source is not allowed and content is of type enhancement, it will be either blocked if content request is new or dropped if content transmission was preempted before.

5.4.5. Departure

When any type of user departs the system, we idle the used frequency. The corresponding link state is updated.

5.5. Energy Consumption Model

The content retrieval is an energy consuming procedure. For energy efficiency, our aim is to minimize the energy consumed per each successfully sent bit over the system.

Table 5.3: Energy model parameters.

Parameter	**Value**	**Parameter**	**Value**
P_{sat}^{total}	240 W	$E_{D,sw(s)}^{rec}$	$P_{dev}^{rec^{sat}} \times \frac{1}{S} \times 0.5$
P_{BS}^{total}	60 W	$E_{D,sw(t)}^{rec}$	$P_{dev}^{rec^{ter}} \times \frac{1}{T} \times 0.2$
P_{sat}^{ch}	$\frac{P_{sat}^{total}}{S}$	$E_{D,sw(t)}^{tx}$	$P_{dev}^{tx} \times \frac{1}{T} \times 0.3$
P_{BS}^{ch}	$\frac{P_{BS}^{total}}{T}$	$E_{D,sw(s->t)}^{rec}$	$3 \times (P_{dev}^{rec^{sat}} \times 0.5)$
P_{dev}^{tx}	80 mW	$E_{D,sw(s->t)}^{tx}$	$3 \times (5 \times P_{dev}^{tx} \times 0.3)$
$P_{dev}^{rec^{sat}}$	$\frac{P_{dev}^{tx}}{5}$	$E_{D,sw(t->s)}^{rec}$	$E_{D,sw(s->t)}^{rec}$
$P_{dev}^{rec^{ter}}$	$\frac{P_{dev}^{tx}}{10}$	$E_{w(s)}^{rec}$	$\frac{E_{D,sw(t->s)}^{rec}}{5}$
P_{dev}^{idle}	$\frac{P_{dev}^{tx}}{20}$	$E_{w(t)}^{rec}$	$\frac{E_{D,sw(s->t)}^{rec}}{5}$
P_{dev}^{sleep}	$\frac{P_{dev}^{tx}}{50}$	$E_{w(t)}^{tx}$	$\frac{E_{D,sw(s->t)}^{tx}}{5}$
P_{BS}^{idle}	$\frac{P_{BS}^{ch}}{20}$	$E_{w(idle)}$	$\frac{\min\{E_{w(s)}^{rec} E_{w(t)}^{rec}, E_{w(t)}^{tx}\}}{2}$
P_{BS}^{sleep}	$\frac{P_{BS}^{ch}}{50}$	$< t_{out}^{dev} >$	$\frac{T}{500}$ sec
$< t_{out}^{BS} >$	$20 < t_{out}^{dev} >$ sec		

To be able to investigate energy consumptions, first let us build energy consumption model for each HU device and the BS. Since the satellite can get the energy from the solar power for communications, we ignore the energy consumption of the satellite.

Since the energy consumption entails the transmission, idling and sleeping powers, receive energy of HU devices retrieving content from the satellite link or the terrestrial link, HU device mode switching and frequency switching energies, wakeup energies for content transmission or retrieval are required as parameter shown in Table 5.3.

5.5.1. HU Device Energy States

For the energy model, we consider the radio frequency (RF) front-end energy, rather than the overall HU device energy consumption such as processing or other activities. Each HU device starts in the sleep state. The sleeping energy consumption is $P_{dev}^{sleep} \times \Delta t_{sleep}$ shown as the loop of the State 1 in Figure 5.3. It wakes up to receive or transmit content shown by the transitions from State 1 to State 2, 3 or 4 in Figure 5.3. The relevant energy consumption is given on the transition arrow. For instance, if the HU device wakes up to receive content from the satellite, it will consume $E_{w(s)}^{rec}$ energy for the wakeup as shown on the transition arrow from State 1 to State 2. Content transmission power is higher compared to content retrieval power and content retrieval power via the satellite link is higher compared to the content retrieval power via the terrestrial link. Let us give an example of the energy consumption during content transmission or retrieval. For instance, if the HU device wakes up to receive content from the satellite it consumes $P_{dev}^{rec^{sat}} \times \Delta t_{rec}^{sat}$ energy shown as the loop of the State 2 in Figure 5.3. After the content transmission or retrieval, HU device transits to idle state shown by the transitions from State 2, 3 or 4 to 5 in Figure 5.3. At State 5, the HU device consumes $P_{dev}^{idle} \times \Delta t_{idle}$ energy for idling. The HU device looks up for the timeout duration. If the time expires, it goes back to the sleep state as shown from State 5 to State 1 in Figure 5.3. If the content transmission or retrieval starts before the time expires, the RF switches either frequency or mode for content transmission or retrieval which corresponds to transitions from the State 5 to State 2, 3 or 4 shown in Figure 5.3. Mode switching means the previous transmission or retrieval of a content was at some link but the new one is at another link. For instance, the previous retrieval of a content was at the terrestrial link but the new one is at the satellite link. Frequency switching means previous and new links are the same but content will be transferred through a

new frequency. The mode switching energy is higher compared to frequency switching energy. For instance, HU device is idling and a new content is to be received by the HU device from the terrestrial link. The previous link was the satellite link. This corresponds to the transition from State 5 to 2 via the transition arrow having energy consumption $E^{rec}_{D,sw(t->s)}$. If a new content request arrives while HU RF frontend is sleeping but the request is blocked, RF transits from the sleep state to the idle state which corresponds to state transition from State 1 to State 5 shown in Figure 5.3.

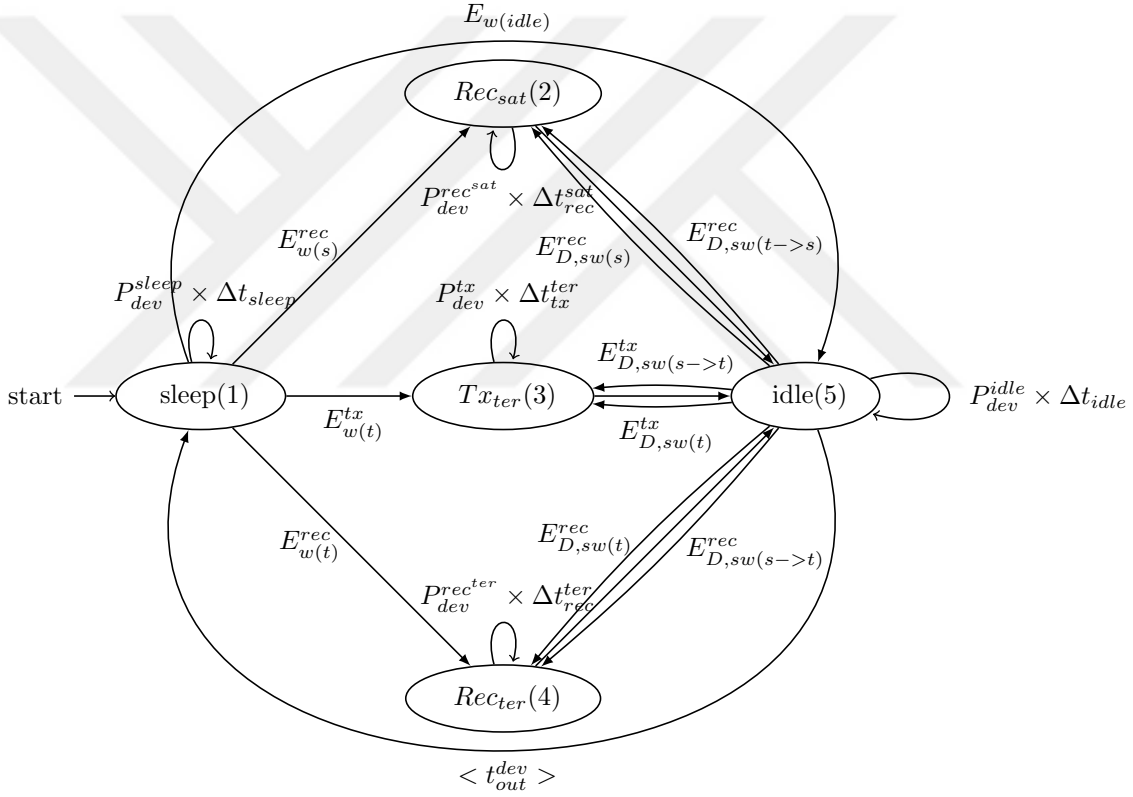


Figure 5.3: HU device energy states.

5.5.2. BS Energy States

We consider the sleep, idling and transmission energy consumptions for BS energy consumption calculation. We ignore the costs of wakeup and switching since it is usually in active mode for continuous operation such controlling network modes and cognitive operation support.

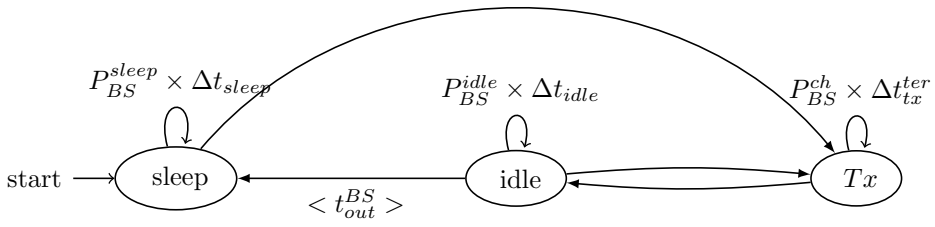


Figure 5.4: BS energy states.

Initially the BS is in the sleep state. The sleeping energy consumption is $P_{BS}^{sleep} \times \Delta t_{sleep}$ shown as the loop of the State 1 in Figure 5.4. When at some terrestrial frequency the BS starts a content transmission, it will transit to transmission state. During content transmission, the BS consumes $P_{BS}^{ch} \times \Delta t_{tx}^{ter}$ energy per each terrestrial frequency. We consider the transmissions where the receiver is an HU device for the calculations. Before the content transmission ends, if another transmission starts at some other frequency, the BS stays at the transmission state. If all the frequencies become idle the BS transits to the idle state. The BS will consume $P_{BS}^{idle} \times \Delta t_{idle}$ energy for idling shown in Figure 5.4. The BS will look up for the timeout duration. If the time expires, it goes back to the sleep state. If content transmission starts before the time expires, the BS transits to transmission state.

5.6. Quality Model

For performance investigation, we also consider a compact content quality model corresponding to the quality experienced by the users (benefit) for layered content operation (base and enhancement layers). In our quality model, we denote the quality indicator value by Q. For each generated HU base content request, we assign a quality indicator value and take their average in the end. If the base content is blocked or dropped then it has quality value zero. If it is served then it has quality value one. After each base content request we investigate the contribution of corresponding enhancement content. If there is no enhancement content generated then current quality indicator value of the base content remains the same. Otherwise, we look at the enhancement content. If it is blocked then current quality indicator value remains the same. If

it is dropped the quality indicator will be added the rate of content size that has been transmitted successfully. For instance, if 40% of the enhancement content is transmitted properly, value 0.4 will be added to current quality indicator value of the corresponding base content. If it is served, then one will be added to current quality indicator value of the corresponding base content. Note that if the base content is dropped it has no positive contribution to the quality. However, the enhancement content has a contribution even if it is dropped.

5.7. Experimental Results

In the simulations, we investigate the performance metrics throughput, energy consumption per successfully sent bit (EPS), i.e. energy efficiency, drop and block rates of HUs and quality. For each case,10 simulations are run and their average is taken as the final result. We perform experiments for different network densities, mode preferences, PU traffic activity, content size, and content popularity characteristics.

5.7.1. Network Density

For different network densities (normal versus sparse), we see that energy consumption per successfully sent bit for HUs is higher in normal networks as shown in Figure 5.5 compared to sparse networks. In normal networks there are more HU devices so the probability of finding content at an HU device increases. As D2D activity increases, since HU devices consume the least transmission energy in the system the energy efficiency is improved. Due to increased D2D activity, energy consumption of HU devices is higher in normal networks as shown in Figure 5.5. In normal networks since there are more HU devices the probability of finding content at some HU device increases and D2D is much more preferred. So, the BS will consume less energy in normal networks compared to sparse networks as shown in Figure 5.5.

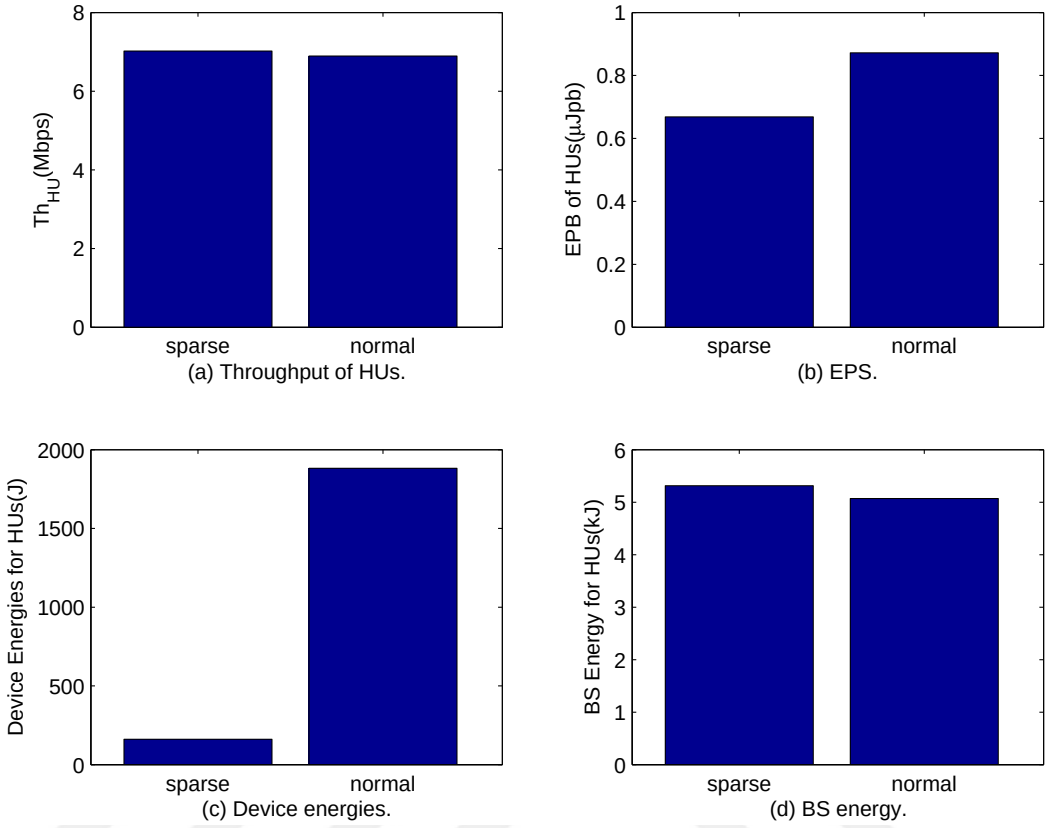


Figure 5.5: Effect of network density on the performance metrics.

The dropping and blocking probability of content requests of HUs is lower in normal networks as shown in Figure 5.6. Since D2D is much more preferred and D2D activities take shorter time , the probability of a new arrived or previously interrupted content request of some HU finding idle frequency in the system increases. As less dropping and blocking occurs in the system, the quality indicator has greater value in normal networks. The average D2D distance is higher in sparse networks since there are less devices throughout the system and the probability of finding a device storing requested content in close proximity is lower.

The density of the network has a positive effect on D2D operation. Although the case for dense and very dense networks is expected to be different due to the increased interference and communication overhead, experimental results in our current settings indicate the advantage of D2D using spatial proximity for system performance.

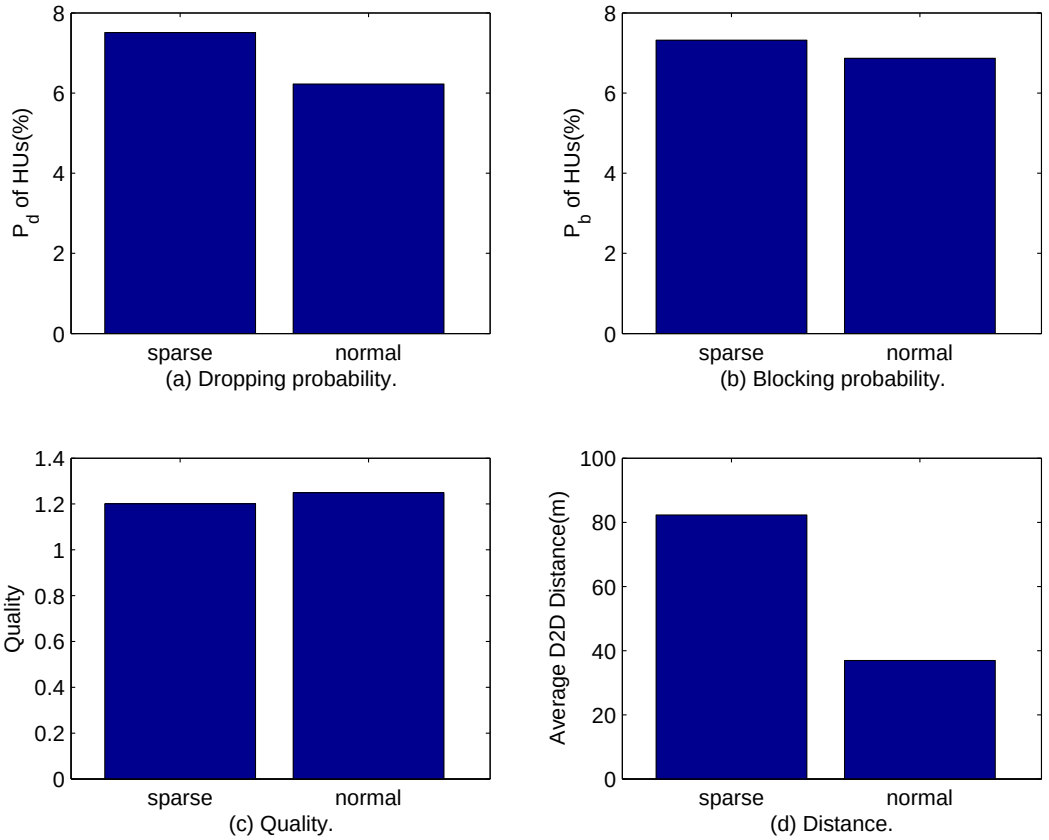
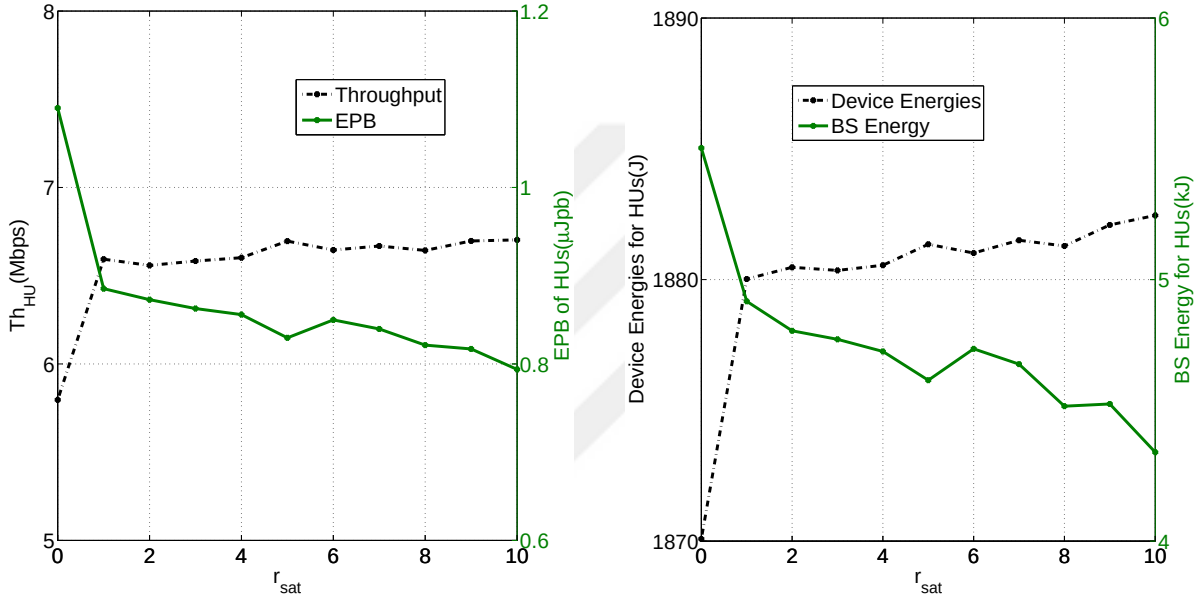


Figure 5.6: Effect of network density.

5.7.2. Effect of Mode Preference: Satellite, BS or D2D

If we introduce the satellite as a part of our system, the throughput is increased as shown in Figure 5.7(a). The satellite channel capacity is typically lower than terrestrial channel capacities. Therefore, services take longer durations compared to terrestrial parts. However, a channel becomes a candidate for new services after it becomes idle. Making satellite preference higher makes the satellite channel saturated by services. So, the system does not improve any further in terms of the throughput. When the satellite preference coefficient is zero, only BS and HU devices can provide content delivery. Hence, introducing the satellite as a part of our system, some of the services will be provided by the satellite but will not result in energy consumption. Hence, there is improvement in energy efficiency as shown in Figure 5.7(a). Note that increasing satellite preference makes the satellite channel saturated by services. So, the system does not improve any further in terms of energy efficiency. Increased satellite preference

coefficient means that the ratio of content retrievals of HUs from the satellite increases which have long service durations. Hence, content-retrieving HU devices stay in receive state instead of sleeping or idling states for longer periods of time and the HU energy consumption increases. Increased satellite preference coefficient leads to decreased BS preference for HU content retrievals. Hence, the energy consumption of the BS for HUs is decreased as given in Figure 5.7(b).

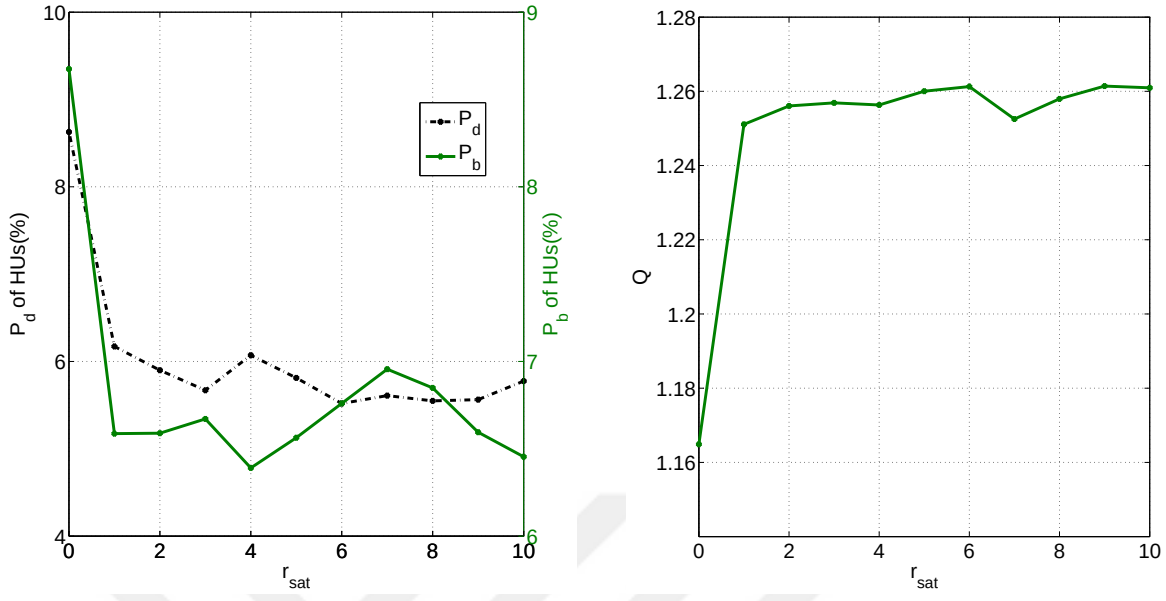


(a) Throughput and EPB.

(b) Energies.

Figure 5.7: Effect of increasing satellite preference parameter.

When we simulate our system with no satellite activity for HUs, we see that the dropping and blocking probabilities of HUs are higher as shown in Figure 5.8(a). When there is no satellite in the system, in case all the terrestrial frequencies are busy there is no satellite frequency option. Therefore, a new content request is blocked. Moreover, in case a PU appears at some terrestrial frequency if there is no idle terrestrial frequency, then the service cannot be continued at the satellite link. Hence, dropping occurs. With the introduction of the satellite into the system, there is an improvement in the content quality as shown in Figure 5.8(b).

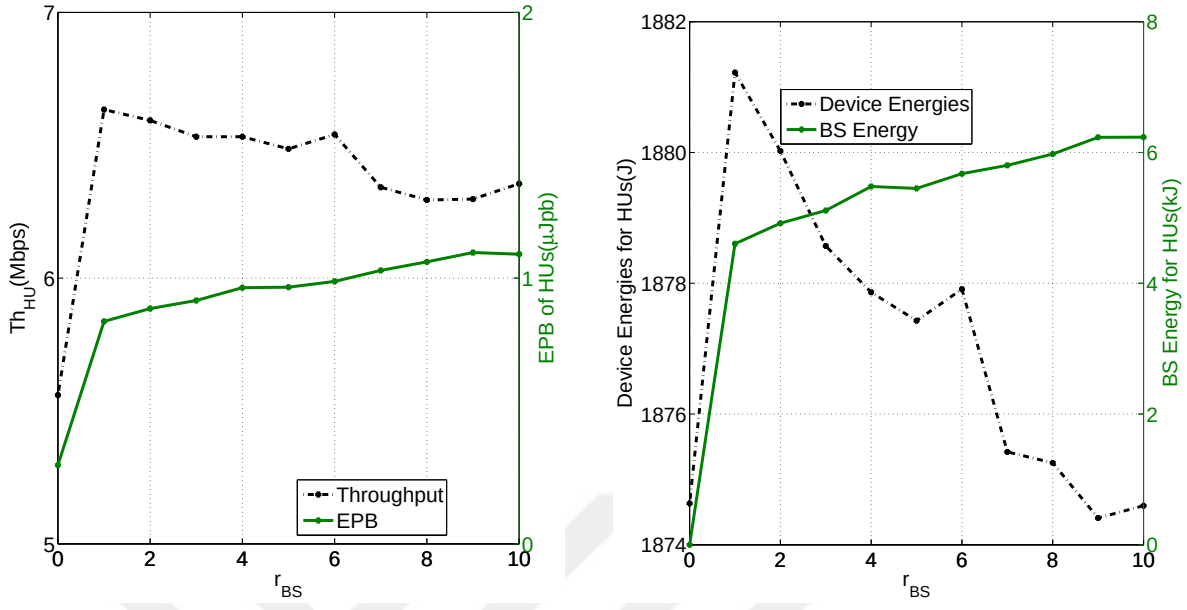


(a) Dropping and blocking probabilities of HUs.

(b) Quality.

Figure 5.8: Effect of increasing satellite preference parameter.

When BS preference coefficient is zero, throughput is low as shown in Figure 5.9(a). With introducing the BS into our system, throughput is improved since the satellite preference is decreased and some of the services taken through the satellite are shifted to the BS mode. The BS is better in terms of potential channel capacity compared to the satellite. Hence, with shorter service durations the system is capable of serving higher number of HUs. Increasing BS preference coefficient to a further extent has negative effect in terms of throughput since this time D2D activity is suppressed. For the energy consumption we ignore the satellite since it can utilize the solar power for communications. As BS preference increases, D2D preference decreases leading to a negative effect on the energy efficiency as shown in Figure 5.9(a). The reason is that D2D mechanism provides better channel capacity with less energy consumption. When BS preference coefficient is zero, total energy consumed by the HU devices is low as shown in Figure 5.9(b). BS preference increase leads to increased energy consumption of the BS for HUs as shown in Figure 5.9(b).

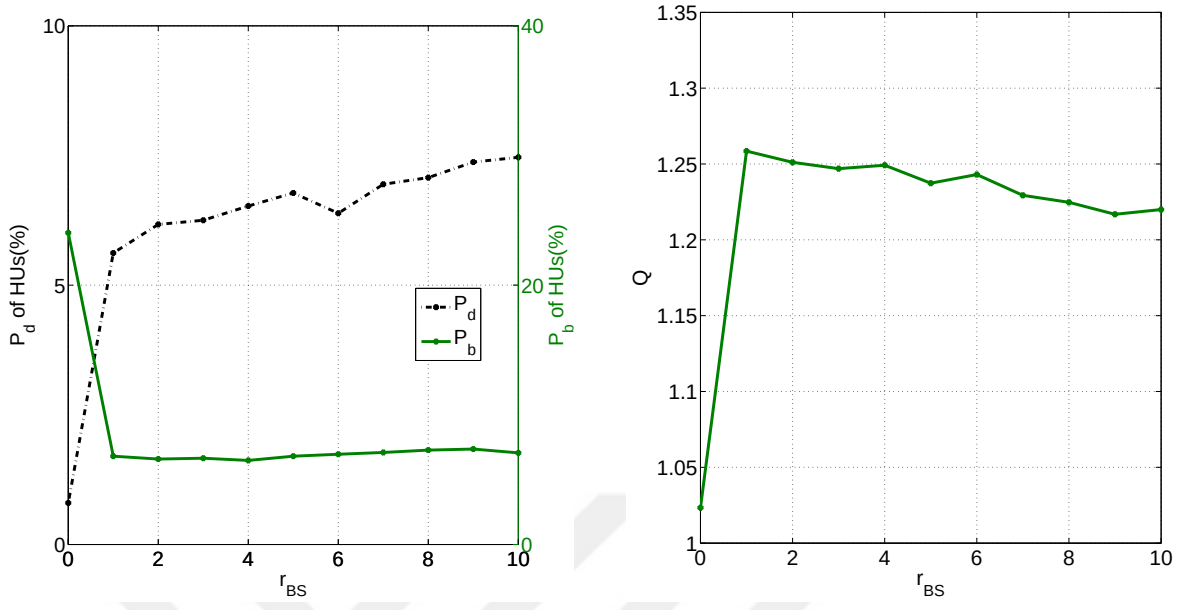


(a) Throughput and EPB.

(b) Energies.

Figure 5.9: Effect of increasing BS preference parameter.

Increasing BS preference coefficient leads to longer content retrieval durations at the terrestrial link and hence the probability of PU arrival during content transmission is increased. Hence the dropping probability of HUs increases as shown in Figure 5.10(a). The blocking probability of HUs is higher when BS activity is not allowed for HUs. The satellite and D2D preferences are higher. The satellite link has higher impact and hence due to longer service durations at the satellite link, the probability of finding idle frequency at the satellite link at some instant of time is lower compared to the terrestrial link. So, the blocking probability is higher in case no BS allowed for HU activity as shown in Figure 5.10(a). When BS is not active, HU block rate is high. Thereof the quality indicator has very low value. When BS becomes active there is a leap in the quality indicator value as shown in Figure 5.10(b). As the dropping rate increases with further increase in the BS preference coefficient value from one to ten the quality indicator value decreases given in Figure 5.10(b).

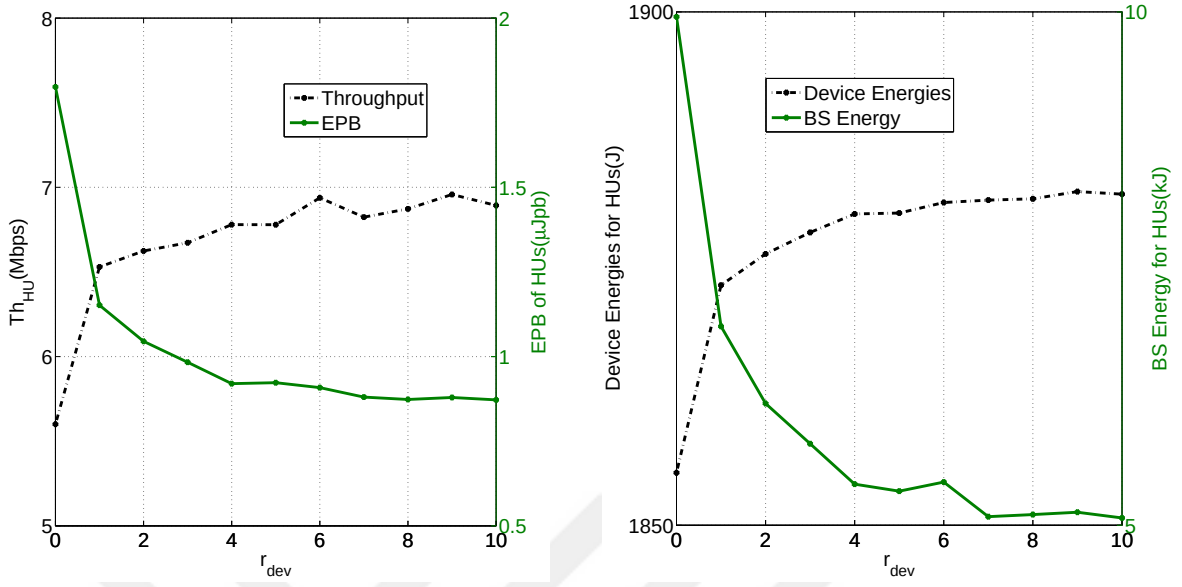


(a) Dropping and blocking probabilities of HUs.

(b) Quality.

Figure 5.10: Effect of increasing BS preference parameter.

An increase in D2D preference leads to shorter content transmission durations of HUs. Hence more requests can be served by the system successfully and the throughput improves as shown in Figure 5.11(a). The increase in the D2D preference coefficient leads to less energy consumption per successfully sent bit over the system. The reason is that the D2D mechanism activity is increased and devices consume less energy compared to other system components. Hence the energy efficiency improves as shown in Figure 5.11(a). As D2D is more preferred, energy consumption of BS decreases whereas energy consumption of HU devices increase as can be seen from Figure 5.11(b). In other words, the energy consumption is offloaded to HUs, i.e. end-devices.

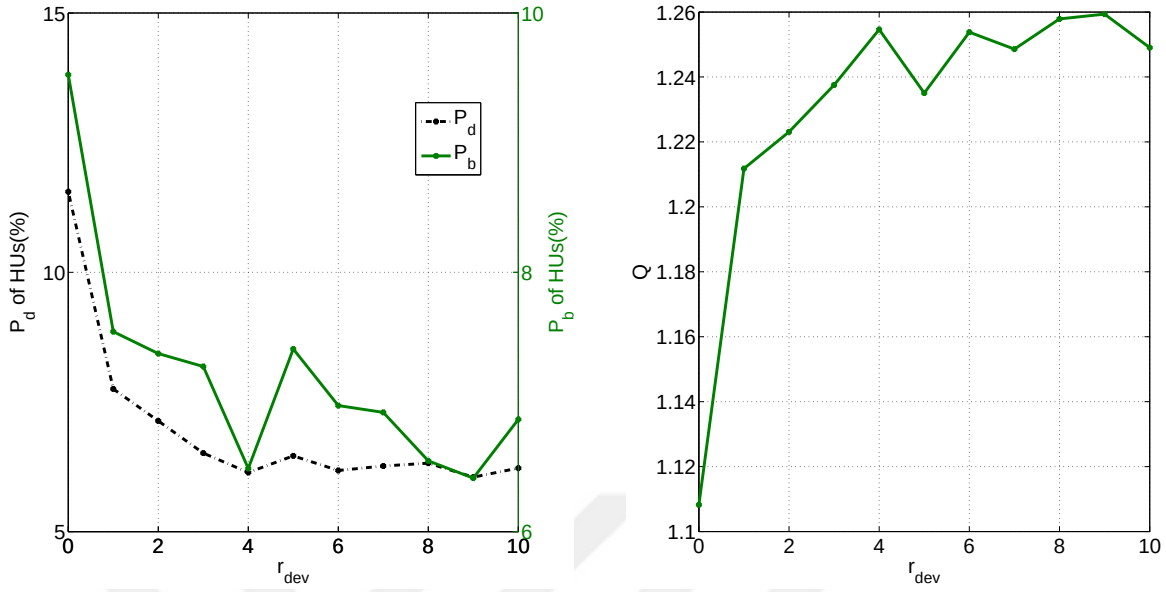


(a) Throughput and EPB.

(b) Energies.

Figure 5.11: Effect of increasing D2D preference parameter.

Increasing D2D preference coefficient leads to shorter content retrieval durations and hence the probability of PU arrival during content transmission is decreased. Then the dropping probability of HUs decreases as shown in Figure 5.12(a). Increasing D2D preference coefficient makes transmission durations of HUs shorter which makes the system having less number of busy channels at an arbitrary instant of time. Consequently, the probability of blocking of HUs decreases as shown in Figure 5.12(a). With increasing D2D preference coefficient, there is a decrease in dropping and blocking rates. This characteristic provides an improvement in the content quality as shown in Figure 5.12(b). From Figure 5.12(a) we can see that there is a local maximum in blocking rate of HUs. Thereof, there is a local minimum for the quality indicator at D2D preference coefficient five as can be seen in Figure 5.12(b).



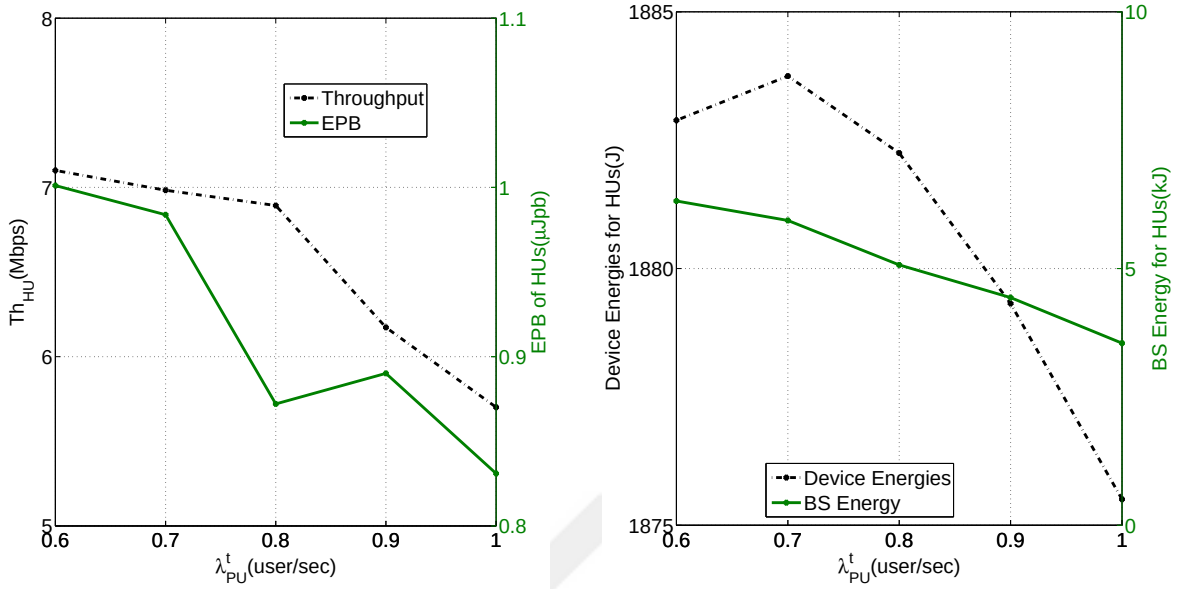
(a) Dropping and blocking probabilities of HUs.

(b) Quality.

Figure 5.12: Effect of increasing D2D preference parameter.

5.7.3. Effect of PU Traffic Activity at Terrestrial Link (Changing $\lambda_{\mathbf{PU}}^{\mathbf{ter}}$)

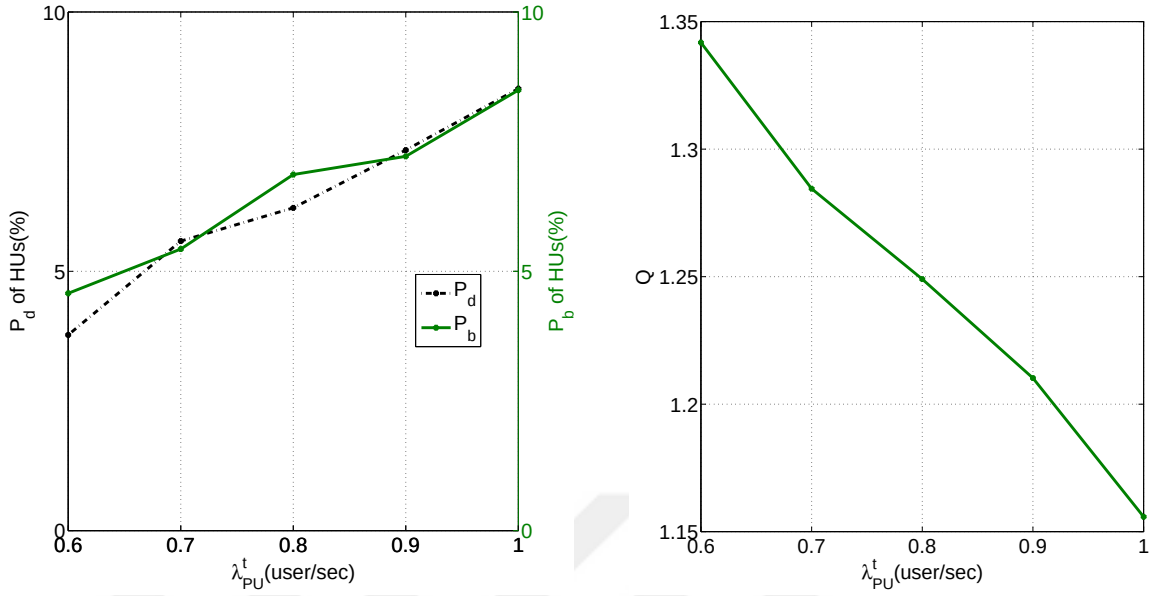
When the arrival rate of PUs at the terrestrial link increases, the resource allocation will prefer more of the satellite frequencies. Since the satellite link has lower channel rate, the content retrievals take longer time in the satellite channel and therefore the overall throughput of HUs decreases as shown in Figure 5.13(a). As the resource allocation will prefer more of the satellite frequencies with increase in the arrival rate of PUs at the terrestrial link, the energy efficiency improves as shown in Figure 5.13(a). However, as the throughput is decreasing this is not a favorable situation. The energy consumption of HU devices and the BS decrease as shown in Figure 5.13(b). The resource allocation preference shifts to the satellite mode. Therefore, the BS and D2D modes are less used and the energy consumption of HU devices and the BS decrease.



(a) Throughput and EPB. (b) Energies.

Figure 5.13: Effect of increasing PU arrival rate at terrestrial link.

The dropping and blocking probability of content requests of HUs increases as the arrival rate of PUs at the terrestrial link increases as shown in Figure 5.14(a). The dropping of HUs occurs only in the terrestrial link since HUs are in SU mode in the terrestrial link. As more and more PUs arrive at the terrestrial link, the forced termination of HUs increases which means higher dropping rate. The blocking of HUs occurs for the new content request arrivals. At each instant of time, less idle terrestrial frequencies will be available. The new content requests will prefer the satellite link. The satellite link has also less idle frequencies and therefore the blocking probability of HUs increases. The quality is decreasing with the increase in the PU arrival rate at the terrestrial link as shown in Figure 5.14(b). As the PU arrival rate at the terrestrial link increases, more content requests are blocked and more dropping occurs in the terrestrial link. Hence, the overall quality reduces.



(a) Dropping and blocking probabilities of HUs.

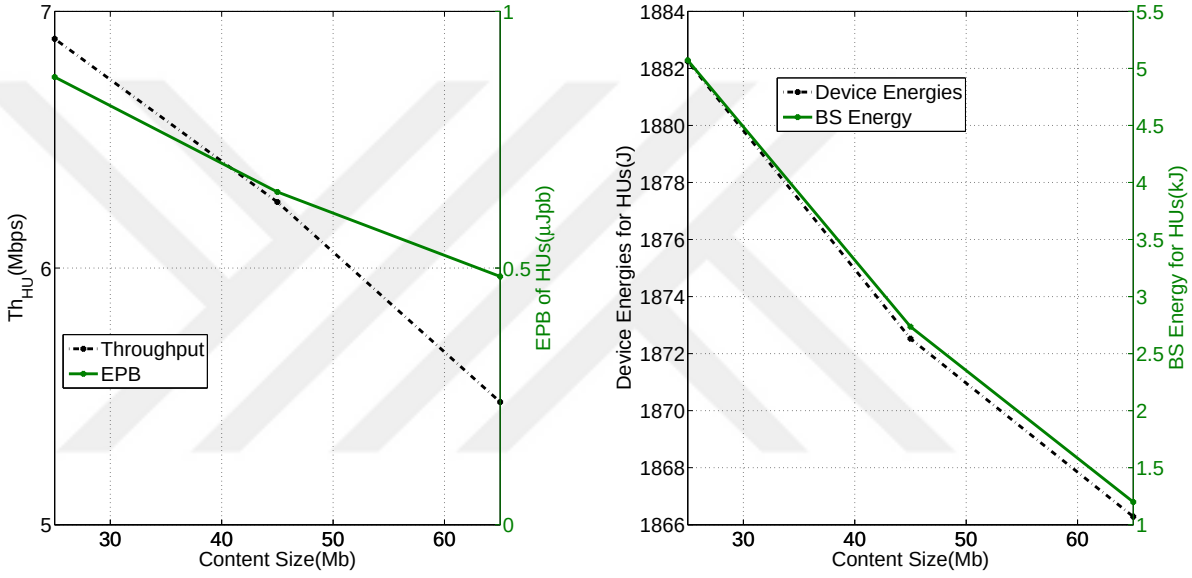
(b) Quality.

Figure 5.14: Effect of increasing PU arrival rate at terrestrial link.

5.7.4. Effect of Content Size

With increasing average content size, the overall throughput of the system is decreased given in Figure 5.15(a). Due to the increased average content size, the service durations become longer. Hence, both the satellite and terrestrial frequencies are in busy state for a longer amount of time. The number of new arrived requests being rejected due to channels being busy increases. Hence the throughput is negatively affected. Additionally, the cache size of all system components is fixed. Hence the satellite, the BS and HU devices all can store less amount of content. The new arrived requests trying to be served via the universal source due to not being found at a cache of system components makes the system much more busy. The throughput is therefore even lower. Also, the energy efficiency is improved that can be seen in the Figure 5.15(a). However, the decrease in the system throughput makes the improvement in the energy efficiency practically useless. With increasing average content size, the energy consumption of both the BS and the HU devices decreas as shown in Figure 5.15(b). The cache size of the BS and HU devices is fixed in the system. When the average content size is increased, they can store less content and hence they can serve

less HU content requests. Also, HU devices can receive less service. Hence both the BS and HU devices consume less energy with increased average content size as shown in Figure 5.15(b).

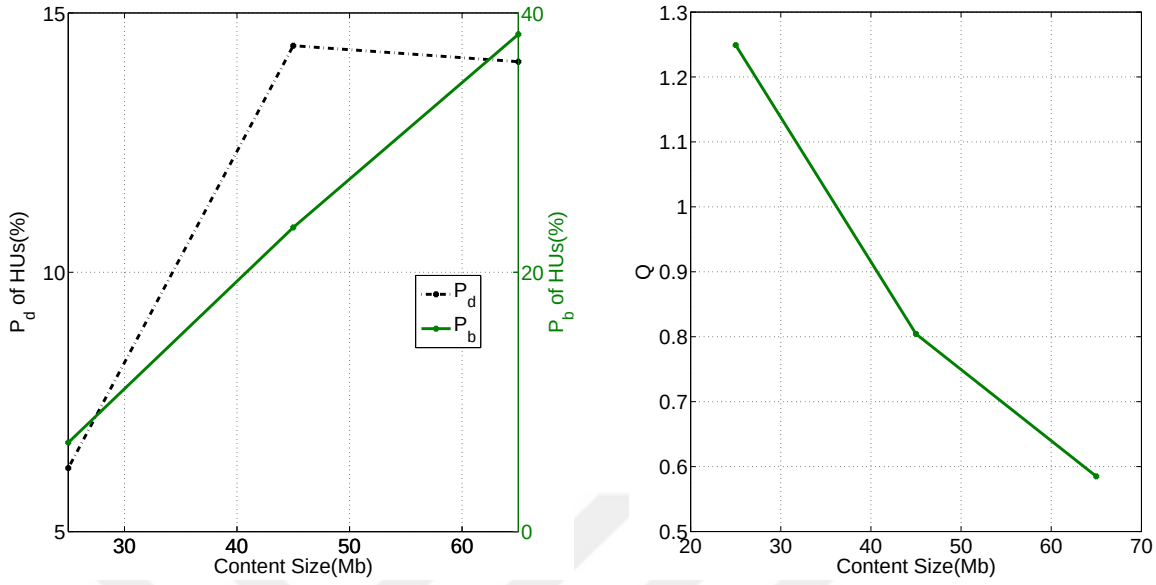


(a) Throughput and EPB.

(b) Energies.

Figure 5.15: Effect of increasing average content size.

We vary average content size for investigating the effect of content size distribution. Increased content size means longer service durations. Longer service duration leads to higher probability of PU appearance at a frequency at the terrestrial link. Keeping other parameters fixed the change on the content size leads to an increase in dropping probability as shown in Figure 5.16(a). Additionally, longer service duration leads to less number of idle frequencies in the system at any instant of time. Hence, the blocking probability of new content request arrivals of HUs to the system increases as shown in Figure 5.16(a). When content size increases, blocking rate increases very rapidly. Thereof, there is a steep decrease in the quality indicator value as given in Figure 5.16(b).



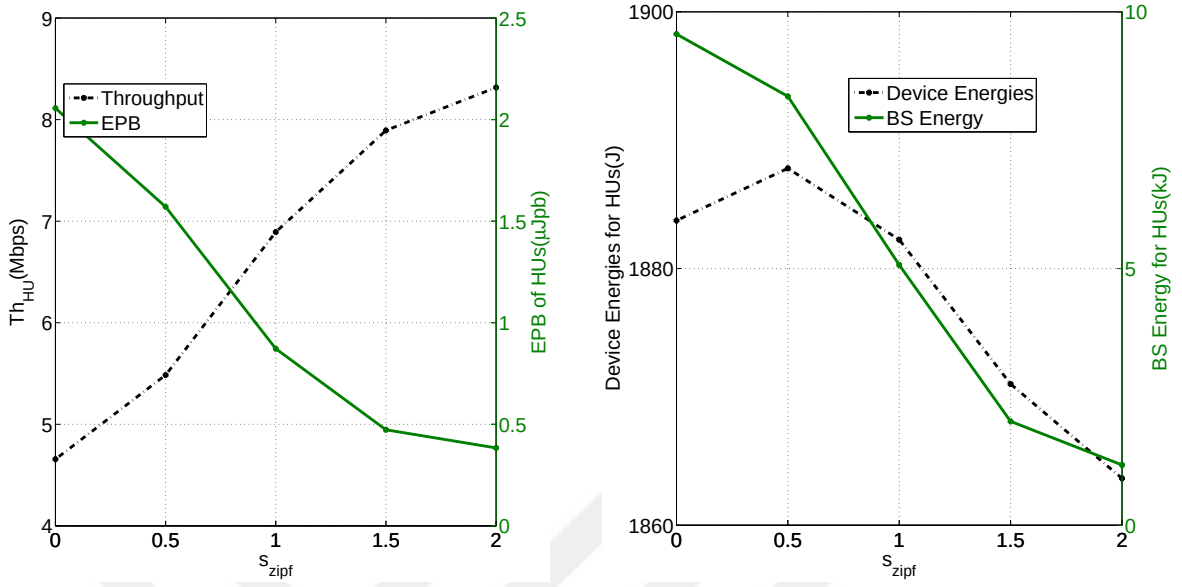
(a) Dropping and blocking probabilities of HUs.

(b) Quality.

Figure 5.16: Effect of increasing average content size.

5.7.5. Effect of Content Popularity Characteristics

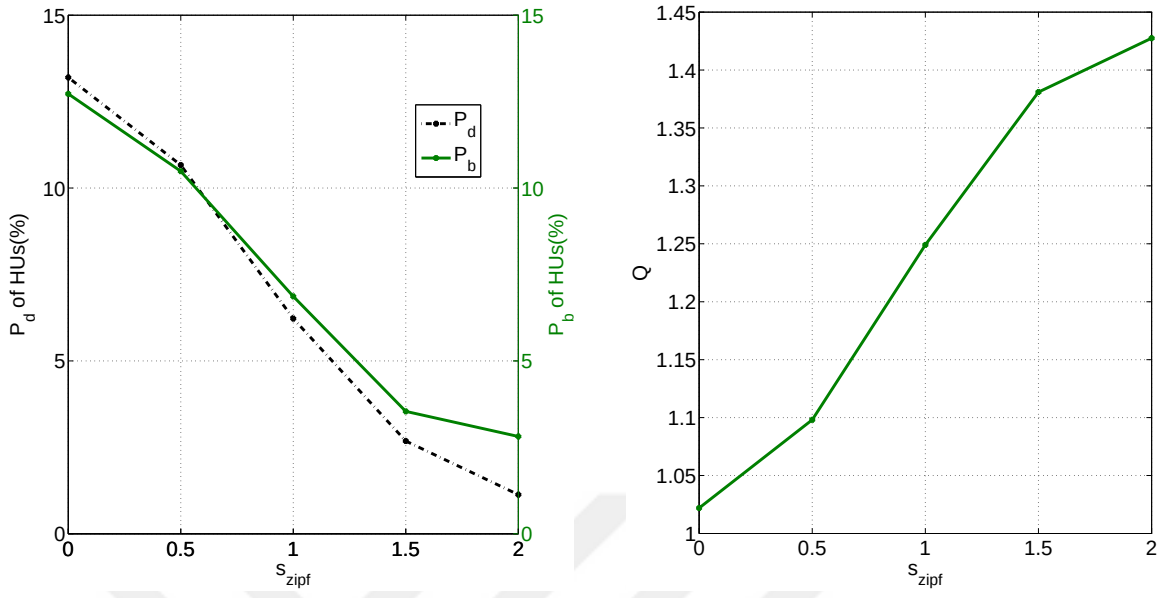
For the content popularity modeling, the Zipf distribution is used as explained in Section 5.1. The Zipf parameter is used to change the popularity distribution among all contents throughout the system. Zipf parameter having value zero means all the contents have the same popularity. With the increase in Zipf parameter, the popularity differentiation is increased. As the popularity differentiation is increased, more popular contents will be requested widely and hence they will be cached in more HU devices. As shown in Figure 5.17(a), the throughput of HUs is increased. The energy efficiency is also improved as shown in Figure 5.17(a) because as more and more HU devices cache popular contents, the probability of finding those contents at closer HU devices increases. Hence, the content transmission via D2D takes shorter time for the same amount of information. i.e. energy efficiency is improved. The energy consumption of HU devices reduces due to the same reason as shown in Figure 5.17(b). As shown in Figure 5.17(b) the energy consumption of the BS reduces since the content availability at HU devices increases.



(a) Throughput and EPB. (b) Energies.

Figure 5.17: Effect of increasing Zipf parameter α value (changing popularity characteristics).

With increasing Zipf parameter, popular contents are cached at more HU devices and the probability of finding content at some close device increases which leads to shorter content retrieval durations and hence the probability of PU arrival during content transmission is decreased. Hence the dropping rate of HUs decreases as shown in Figure 5.18(a). The shorter content retrieval durations makes the system having less number of busy channels at an arbitrary instant of time. So, the rate of HUs being blocked decreases as shown in Figure 5.18(a). When we increase the zipf parameter, the quality indicator increases as given in Figure 5.18(b). As explained above the dropping and blocking rates reduce with the increasing zipf parameter. Hence, the quality is improved.



(a) Dropping and blocking probabilities of HUs.

(b) Quality.

Figure 5.18: Effect of increasing Zipf parameter α value (changing popularity characteristics).

6. CONCLUSIONS

Most of the CRN resource allocation schemes have focused on throughput or capacity improvement with PU coexistence constraints. However, the energy consumed for content transmission is also a key emerging factor in CRN performance. Although a multitude of works on the energy consumption exist in the literature, the analysis of trade-offs due to various factors are worth research since the reduced energy consumption resulting in poor network performance is not desirable. Additionally, most of the works dwell on on terrestrial CRNs only. The satellite segment integration together with D2D extension in the resource allocation literature is not evident. Moreover, there is the content dimension which is becoming the dominant and challenging traffic component in wireless networks. This phenomenon promotes a content-centric operation mode for wireless networks.

In this thesis, we have investigated the satellite integrated CRN with D2D communications and content-centric operation from the performance perspective. This research is done in two-folds. Firstly, the system is modelled via CTMC. We laid out an analytical model for the system and performed numerical runs for various parameters such as mode preference for content retrieval from different content holders. As the preference shifts to the BS (infrastructure-based transmission) or D2D, the energy efficiency is improved. The improvement of D2D is higher than the BS counterpart due to better channel capacity and less energy consumption of D2D mechanism. The preference shift towards the satellite leads to decreased energy efficiency. However, due to higher cache capacity content availability is the highest among all the content holders for this case. Additionally, the network throughput is increased. Taking all of these into account the network managers should take the preference ratio according to the system requirements. If energy consumption is tolerable, preference shift to the satellite is acceptable. If energy efficiency is the main determinant of the network, preference shift to D2D mechanism is to be chosen. We also simulated this analytical model to investigate the behavior against a simulated analysis. This effort rendered us the capabilities of our model and provided insight for its operation.

Secondly, extensive simulations are done in a simulation environment developed for this system and the energy consumption of HU devices and the BS are modeled extensively. For this latter setup, The increase in D2D preference leads to improved energy efficiency. When the contents are modeled according to a popularity model, the energy efficiency improves as the popularity differentiation is increased. The reason is that if few contents are extremely popular than other contents, then they are available at more content holders and hence they can be retrieved with less energy consumption.

For future work, the layered content concept and content popularity is to be modeled by CTMC. In the simulations, dependency between contents affecting their utility can be integrated. "Universal source" concept which represents the other content holders out of our network scope can be added to the analytical model. In network layout, overlay mechanism for D2D can be investigated in terms of energy efficiency. The multicast nature of satellite can be used for further improvements due to satellite integration into the CRN.

REFERENCES

1. Ghasemi, A. and E. Sousa, "Spectrum sensing in cognitive radio networks: requirements, challenges and design trade-offs", *Communications Magazine, IEEE*, Vol. 46, No. 4, pp. 32–39, April 2008.

2. Wang, C.-X., F. Haider, X. Gao, X.-H. You, Y. Yang, D. Yuan, H. Aggoune, H. Haas, S. Fletcher, and E. Hepsaydir, "Cellular architecture and key technologies for 5G wireless communication networks", *Communications Magazine, IEEE*, Vol. 52, No. 2, pp. 122–130, February 2014.

3. Adigun, O., M. Pirmoradian, and C. Politis, *Cognitive Radio for 5G Wireless Networks*, pp. 149–163, John Wiley & Sons, Ltd, 2015.

4. Asadi, A., Q. Wang, and V. Mancuso, "A Survey on Device-to-Device Communication in Cellular Networks", *Communications Surveys Tutorials, IEEE*, Vol. 16, No. 4, pp. 1801–1819, Fourthquarter 2014.

5. Sambo, Y., M. Shakir, K. Qaraqe, E. Serpedin, M. Imran, and B. Ahmed, "Energy efficiency improvements in HetNets by exploiting device-to-device communications", *Signal Processing Conference (EUSIPCO), 2014 Proceedings of the 22nd European*, pp. 151–155, Sept 2014.

6. ITU-R SG05, "M.2320 Future technology trends of terrestrial IMT systems", Technical report, International Telecommunication Union (ITU), Geneva, 2014.

7. Paper, C. W., "Cisco Visual Networking Index: Global Mobile Data Traffic Forecast Update, 2014-2019", February 2015.

8. Gür, G., "Energy-aware cache management at the wireless network edge for information-centric operation", *Journal of Network and Computer Applications*, Vol. 57, pp. 33 – 42, 2015.

9. Shah, G., F. Alagoz, E. Fadel, and O. Akan, "A Spectrum-Aware Clustering for Efficient Multimedia Routing in Cognitive Radio Sensor Networks", *Vehicular Technology, IEEE Transactions on*, Vol. 63, No. 7, pp. 3369–3380, Sept 2014.

10. Alagoz, F. and G. Gur, "Energy Efficiency and Satellite Networking: A Holistic Overview", *Proceedings of the IEEE*, Vol. 99, No. 11, pp. 1954–1979, Nov 2011.

11. Evans, B., "The role of satellites in 5G", *Advanced Satellite Multimedia Systems Conference and the 13th Signal Processing for Space Communications Workshop (ASMS/SPSC), 2014 7th*, pp. 197–202, Sept 2014.

12. Bayhan, S., G. Gur, and F. Alagoz, "High Altitude Platform (HAP) Driven Smart Radios: A Novel Concept", *Satellite and Space Communications, 2007. IWSSC '07. International Workshop on*, pp. 201–205, Sept 2007.

13. Gur, G. and F. Alagoz, "Energy-efficient layered content dissemination for multimode mobile devices", *Communications and Networking (BlackSeaCom), 2013 First International Black Sea Conference on*, pp. 243–246, July 2013.

14. Bayhan, S., S. Eryigit, and G. Gur, "Energy efficiency in Cognitive Radio Networks: Challenges, Trade-offs, and Solutions", Tutorial presented as the CROWNCOM 2015, Doha, Qatar, 2015.

15. Eryigit, S., G. Gur, S. Bayhan, and T. Tugcu, "Energy efficiency is a subtle concept: fundamental trade-offs for cognitive radio networks", *Communications Magazine, IEEE*, Vol. 52, No. 7, pp. 30–36, July 2014.

16. Gür, G. and F. Alagöz, "Green wireless communications via cognitive dimension: an overview", *Network, IEEE*, Vol. 25, No. 2, pp. 50–56, March 2011.

17. Jiang, T., H. Wang, and Y. Zhang, "Modeling Channel Allocation for Multimedia Transmission Over Infrastructure Based Cognitive Radio Networks", *Systems Journal, IEEE*, Vol. 5, No. 3, pp. 417–426, Sept 2011.

18. Wang, H., Y. Qian, and H. Sharif, "Multimedia communications over cognitive radio networks for smart grid applications", *Wireless Communications, IEEE*, Vol. 20, No. 4, pp. 125–132, August 2013.

19. Jounsup Park, J.-N. H., Xiang Chen, "Optimum Power Allocation and Rate Adaptation for Scalable Video Streaming over Multi-User MIMO Networks", *IEEE International Conference on Communications*.

20. Vassaki, S., M. Poulakis, A. Panagopoulos, and P. Constantinou, "Power Allocation in Cognitive Satellite Terrestrial Networks with QoS Constraints", *Communications Letters, IEEE*, Vol. 17, No. 7, pp. 1344–1347, July 2013.

21. Kawamoto, Y., Z. Fadlullah, H. Nishiyama, N. Kato, and M. Toyoshima, "Prospects and challenges of context-aware multimedia content delivery in cooperative satellite and terrestrial networks", *Communications Magazine, IEEE*, Vol. 52, No. 6, pp. 55–61, June 2014.

22. Ge, Y., M. Chen, Y. Sun, Z. Li, Y. Wang, and E. Dutkiewicz, "QoS provisioning wireless multimedia transmission over cognitive radio networks", *Multimedia Tools and Applications*, Vol. 67, No. 1, pp. 213–229, 2013, `http://dx.doi.org/10.1007/s11042-011-0937-4`.

23. Jiang, T., H. Wang, and A. Vasilakos, "QoE-Driven Channel Allocation Schemes for Multimedia Transmission of Priority-Based Secondary Users over Cognitive Radio Networks", *Selected Areas in Communications, IEEE Journal on*, Vol. 30, No. 7, pp. 1215–1224, August 2012.

24. Chu, T. M. C., H. Phan, and H.-J. Zepernick, "Dynamic Spectrum Access for Cognitive Radio Networks with Prioritized Traffics", *Communications Letters, IEEE*, Vol. 18, No. 7, pp. 1218–1221, 2014.

25. Balapuwaduge, I., L. Jiao, V. Pla, F. Y. Li, *et al.*, "Channel assembling with priority-based queues in cognitive radio networks: Strategies and performance

evaluation", *Wireless Communications, IEEE Transactions on*, Vol. 13, No. 2, pp. 630–645, 2014.

26. Tumuluru, V. K., P. Wang, D. Niyato, and W. Song, "Performance analysis of cognitive radio spectrum access with prioritized traffic", *Vehicular Technology, IEEE Transactions on*, Vol. 61, No. 4, pp. 1895–1906, 2012.

27. Gür, G., S. Bayhan, and F. Alagöz, "Hybrid satellite–IEEE 802.16 system for mobile multimedia delivery", *International Journal of Satellite Communications and Networking*, Vol. 29, No. 3, pp. 209–228, 2011.

28. Li, Y., Z. Wang, D. Jin, and S. Chen, "Optimal Mobile Content Downloading in Device-to-Device Communication Underlaying Cellular Networks", *Wireless Communications, IEEE Transactions on*, Vol. 13, No. 7, pp. 3596–3608, July 2014.

29. Ding, G., J. Wang, Q. Wu, Y. Yao, F. Song, and T. Tsiftsis, "Cellular-Base-Station Assisted Device-to-Device Communications in TV White Space", *Selected Areas in Communications, IEEE Journal on*, Vol. PP, No. 99, pp. 1–1, 2015.

30. Chen, X., R. Q. Hu, J. Jeon, and G. Wu, "Energy Efficient Resource Allocation for D2D Communication Underlaying Cellular Network", *Communications (ICC), 2015 IEEE International Conference on*, pp. 1–6, June 2015.

31. Gür, G., S. Bayhan, and F. Alagöz, "Energy Efficiency Impact of Cognitive Femtocells in Heterogeneous Wireless Networks", *Proceedings of the 1st ACM Workshop on Cognitive Radio Architectures for Broadband*, CRAB '13, pp. 53–60, ACM, New York, NY, USA, 2013, `http://doi.acm.org/10.1145/2508478.2508480`.

32. Choi, J., J. Han, E. Cho, T. Kwon, and Y. Choi, "A Survey on content-oriented networking for efficient content delivery", *Communications Magazine, IEEE*, Vol. 49, No. 3, pp. 121–127, March 2011.

33. Jacobson, V., D. K. Smetters, J. D. Thornton, M. F. Plass, N. H. Briggs, and

R. L. Braynard, "Networking Named Content", *Proceedings of the 5th International Conference on Emerging Networking Experiments and Technologies*, CoNEXT '09, pp. 1–12, 2009.

34. Emre, M., G. Gur, S. Bayhan, and F. Alagoz, "CooperativeQ: Energy-Efficient Channel Access Based on Cooperative Reinforcement Learning", *Communications (ICC), 2015 IEEE International Conference on, Workshop on Next Generation Green ICT*, pp. 1–6, June 2015.

35. Evans, B., M. Werner, E. Lutz, M. Bousquet, G. Corazza, and G. Maral, "Integration of satellite and terrestrial systems in future multimedia communications", *Wireless Communications, IEEE*, Vol. 12, No. 5, pp. 72–80, Oct 2005.

36. Wu, D., Y. T. Hou, and Y.-Q. Zhang, "Scalable video coding and transport over broadband wireless networks", *Proceedings of the IEEE*, Vol. 89, No. 1, pp. 6–20, Jan 2001.

37. Wang, L., S. Bayhan, J. Ott, J. Kangasharju, A. Sathiaseelan, and J. Crowcroft, "Pro-Diluvian: Understanding Scoped-Flooding for Content Discovery in Information-Centric Networking", *Proceedings of the 2nd International Conference on Information-Centric Networking*, pp. 9–18, 2015.